Scientific and Technological Alliance for Guaranteeing the European Excellence in Concentrating Solar Thermal Energy

FP7 Grant Agreement number: 609837
Start date of project: 01/02/2014
Duration of project: 48 months

Project Deliverable 9.5:

Final Report on Solar Fuels Activities

WP9 – All Tasks	**Deliverable 9.5**
Due date:	**01/2018**
Submitted	**01/2018**
Partner responsible	**PSI**
Person responsible	**Christian Wieckert**
Author(s):	**Gilles Flamant (CNRS), Alessandro Galia (UNIPA), Manuel Romero (IMDEA), José González (IMDEA), Ronald Michalsky (ETHZ), Luca Turchetti (ENEA), Christian Sattler (DLR), Nathalie Monnerie (DLR), Alfonso Vidal (CIEMAT), Cristina Prieto (ASNT), Paula Costa (LNEG), Christian Wieckert (PSI)**
Document version:	**3**
Reviewed/supervised by:	**ChristianWieckert**
Dissemination Level	**PU**

Table of contents

Figures

Tables

1. Introduction and overview

Research in WP9 of STAGE-STE called "Solar Fuels" is focused on high-temperature thermochemical processes that efficiently convert concentrated solar energy into storable and transportable fuels. In the long term, H_2O/CO_2-splitting thermochemical cycles mainly based on metal oxide redox reactions will be developed to produce H_2 and CO (syngas), which can be further processed to synthetic liquid fuels (e.g., diesel, jet fuel). In the shorter term, carbonaceous feedstock (fossil fuels, biomass, C-containing wastes) is being solar-upgraded and transformed into valuable fuels via gasification and reforming processes.

The objectives of this WP are to further develop and demonstrate the technical and economic feasibility of solar thermochemical processes for the production of fuels, identify main technological challenges and elaborate innovative solutions, perform environmental and economic assessments, and formulate essential R&D requirements for future industrial technology implementation.

Eleven partners have contributed to WP9: CIEMAT, DLR, PSI (coordinating), CNRS, ENEA, ETHZ, LNEG, UEVORA, IMDEA, UNIPA and ASNT. The WP has been organised in four tasks with several subtopics in each task. Two tasks are about the major technologies and solar reactors while the other two are horizontal tasks on materials and on technology assessment. Fig. 1 provides a schematic showing the WP structure and the major activity lines.

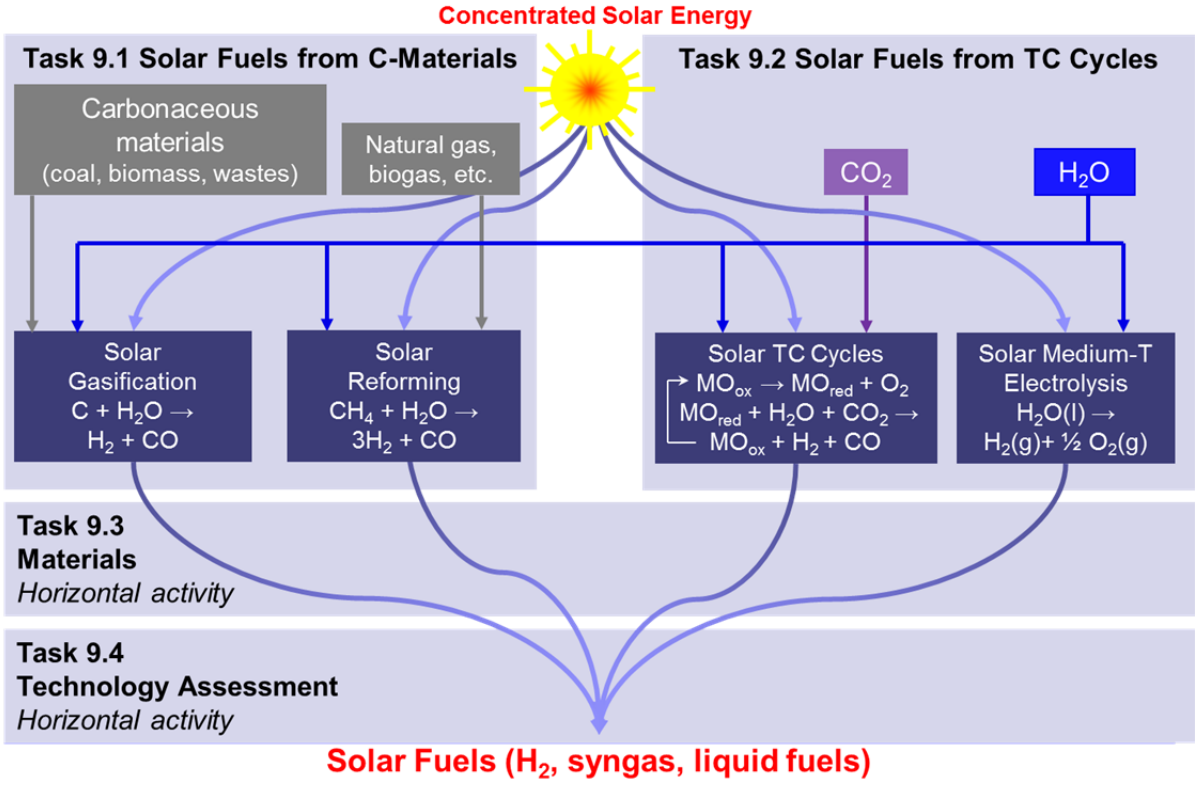

Figure 1. Task-structure of WP9

A total of 199.4 person months have been committed to this WP. Table 1 presents the involvement of the different partners in the different tasks.

Partner short name	Overall PM	Task 9.1	Task 9.2	Task 9.3	Task 9.4
CIEMAT	**11**	**5**	3	2	1
DLR	**36.4**	0	6	0	**30.4**
PSI	**32**	12	**12**	2	6
CNRS	**42**	2	38	**2**	0
ENEA	**15**	6	6	0	3
ETHZ	**4**	2	2	0	0
LNEG	**20**	16	0	4	0
UEVORA	**1**	0	0	0	1
IMDEA	**24**	6	10	4	4
UNIPA	**12**	12	0	0	0
ASNT	**2**	0	2	0	0
TOTAL	**199.4**	**61**	**79**	**14**	**45.4**

Table 1. Person months foreseen by the partners for the different tasks. The PM of the partner leading a task is given in bold.

A total of over 46 person weeks of staff exchange activities have been reported in WP4 related to WP9 (see Table 2). 34.4 weeks thereof were at the visited institutions while 13.3 weeks were remote preparation and evaluation work at the home institutions.

Partner Nr.	To / From	Total weeks outgoing	CIEMAT	DLR	PSI	CNRS	ENEA	ETHZ	LNEG	IMDEA	UNIPA
1	CIEMAT	6				2			4		
2	DLR	0									
3	PSI	4	4								
4	CNRS	2		2							
6	ENEA	0									
7	ETHZ	9								9	
10	LNEG	3.3					1.1				2.2
16	IMDEA	6	1					5			
19	UNIPA	16					16				
	Total weeks incoming	46.3	5	2	0	2	17.1	5	4	9	2.2

Table 2. Overview over staff exchanges between European STAGE-STE partners related to WP9 (performed under WP4 of STAGE-STE)

Two activities involving oversee STAGE-STE partners have been reported in WP6:

(1) Cooperation between UNAM (Mexico), IMDEA and PSI for solar steam gasification of Mexican petcoke. A Ph.D. student from UNAM spent two months at IMDEA for small scale and thermogravimetric tests followed by another three months at PSI for lab scale solar gasification tests in the 5 kW_{th} two-cavity solar reactor.
(2) Exploration by PSI for potential joint pilot scale solar thermochemical reactor testing using the solar tower at CSIRO (Australia). The discussions were discontinued due to the later decision of PSI to phase out of CSP research.

This deliverable report provides a short summary of the work performed within this WP over the total course of the project. Much more details can be found in the four further deliverable reports, the four milestone reports, in the publications that arose from the activities and in further documents and disseminations. Furthermore 30 assets related to WP9 have been added to the EERA IPRepository to date and five partnering opportunities related to WP9 activities are offered so far in the EERA public showcase.

2. Task 9.1 “Solar fuels from carbonaceous feedstock”

In this task led by CIEMAT with further participants PSI, CNRS, ENEA, ETHZ, LNEG, IMDEA and UNIPA near-term processes such as solar steam reforming of natural gas or solar steam gasification of carbonaceous materials have been studied both conceptually and experimentally using solar chemical reactors for different feedstock including coke and various types of biomass. Fundamental work encompassed solar reactor and systems modelling, thermodynamic and kinetic analyses of pertinent chemical processes as well as characterisation of feedstock and products. Further optimization of processes like solar reforming and gasification technologies have been performed in experiments predominantly at laboratory scale (1-10 kW_{th}). For the most advanced processes, input to economic analyses of industrial plants has been generated based on test results and validated reactor models. These analyses have been performed in Task 9.4 as reported in Chapter 5.

A special activity defined within this task was about the investigation of different pyrolysis and gasification processes under development at different partners using the same feedstock. LNEG organised and distributed for this purpose the specific microalgae “Chlorella Vulgaris“. The partners LNEG, UNIPA, CNRS and IMDEA participated in this activity. These comparative tests were performed in the year 2017 and the evaluation of the results is still ongoing.

2.1 Reactor and process modelling

Mostly related to major research activities described in subchapters 2.2, 2.3 and 2.4 numerous modelling activities have been performed with a varying degree of sophistication. Significant respective investigations include the following:

- Modelling for window protection for steam gasification in vortex flow reactor (related to Synpet project)

CIEMAT performed thermal simulations of an aerodynamic curtain to protect the transparent quartz window of the 500 kW_{th} solar reactor designed and fabricated within the SYNPET project [1]. CFD modelling was applied to solve design issues and optimize the solar operating conditions. The selection of the most appropriate operating conditions to avoid particle deposition on the quartz window was based on two criteria: (i) “best” vortex definition and (ii) lowest temperature gradient at the outlet of the reactor pre-chamber. The simulation involves a three-dimensional geometry, which represents the fluid domain corresponding to the conical part in front of the aperture (Figure 2, left). It was observed that the vortex appears only when the mass flow rate of the tangential jets is larger than that of the radial jets. The optimum tangential to radial mass flow ratio was found to be 3 to 1 for this configuration [2].

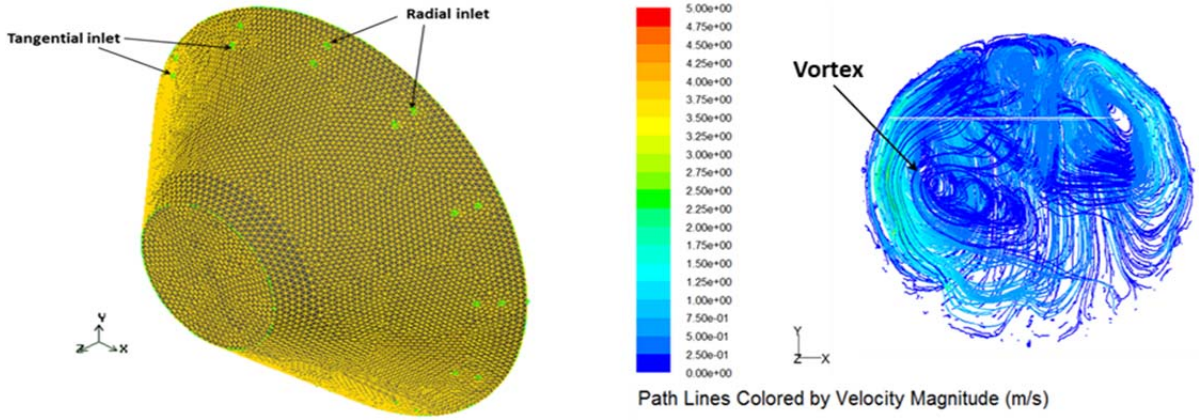

Figure 2. Left: Geometry and mesh of the simulation domain. Right: Evaluation of the predominant inlet flow configuration: mass flow rate = 111 kg/h; tangential/radial mass flow ratio = 3/1. (CIEMAT)

- Modelling of steam gasification in a gas-solid trickle bed reactor (related to Chap. 2.4)

At ETHZ, work was carried out on heat transfer modelling and validation of steam gasification with a drop tube reactor [3]. Beech charcoal particles were used as the model feedstock. A two-dimensional finite-volume model coupling chemical reaction with conduction, convection, and radiation of heat within the packing was developed and tested against measured temperatures and gasification rates. The sensitivity of the gasification rate and reactor temperatures to variations of the packing's pore diameter, porosity, thermal conductivity, and particle loading was numerically studied.

2.2 Solar pilot plant for steam gasification of carbonaceous feedstock

- Pilot plant

The ownership of PSI's 150 kW_{th} pilot solar gasification plant [4] based on the indirectly-heated packed-bed technology and installed on the large tower at the Plataforma Solar de Almeria (PSA) has been transferred to CIEMAT. The know-how transfer was performed during an exchange stay of PSI personal at PSA (mobility activity under Task 4.1). The plant is available for further gasification tests. The significant effort for a reactivation of the pilot plant would require the involvement of a further ideally industrial partner and/or another funding source, which has not been achieved yet.

- Laboratory scale tests for the same packed-bed technology

The 5 kW_{th} lab-reactor (Fig. 3) was used to study the steam gasification of petcokes from Mexico. This activity has been performed in cooperation with UNAM (Mexico) and IMDEA and was hence also related to Task 6.3.3. Solar steam gasification of different petcokes was successfully demonstrated using PSI's high flux solar simulator. Figure 4 shows the results of a typical test in which 300 g of Mexican petcoke were converted to a synthesis gas and 10 g ash residue. The solar upgrade, defined as LHV of produced syngas divided by LHV of feedstock, was about 1.2.

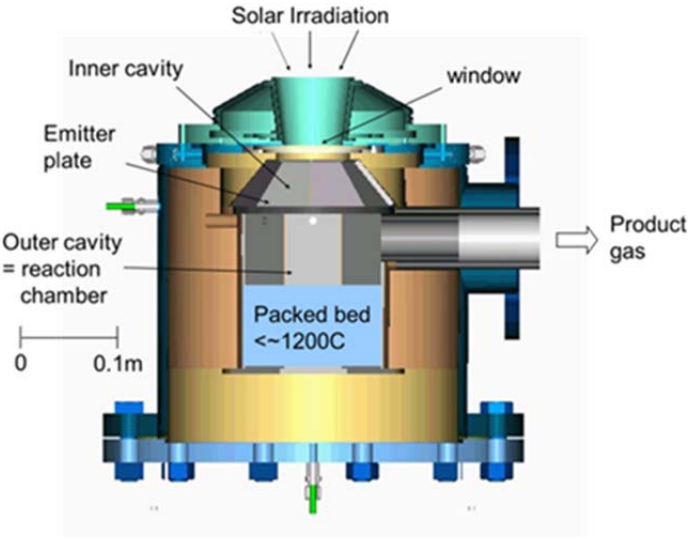

Figure 3. 5 kW_{th} laboratory packed-bed lab-reactor at PSI

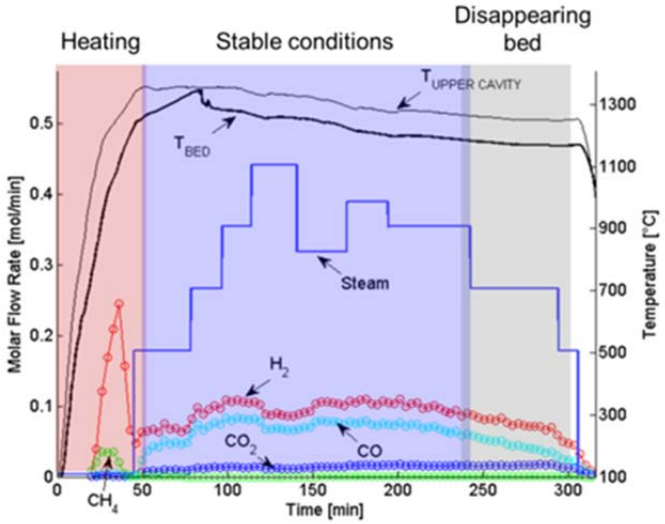

Figure 4. Temperatures and gas compositions during typical gasification experiment with packed bed of petcoke

In the framework of an Indo-Swiss research project with ETHZ as Swiss partner ETHZ/PSI used the same two-cavity 5 kW laboratory scale solar reactor (Fig. 3) heated by the High Flux Solar Simulator to steam gasify soybean husk, black mustard husk and straw, and cotton bolls [5]. The objectives of the tests were to convert the agricultural wastes into solar upgraded synthesis gas and to recover the contained potassium for reuse as fertilizer. The tests were successful and several 100 g of feedstock per test were converted within 1-2 hours. The fate of the potassium was investigated as a function of the gasification temperature. Potassium-concentrations of up to 25% were found in the residues, either the ash (at temperatures below 1100°C) or in the condensate from the offgas system (at higher temperatures).

2.3 Fundamental investigation of solar biomass gasification

- Pyrolysis and gasification tests in small directly irradiated packed bed/crucible reactor

IMDEA investigated the pyrolysis of low-grade biomass at solar-simulator scale [6, 7]. First three low-grade carbonaceous, non-food competitive, feedstock materials were selected: green microalgae of type Scenedesmus, municipal sewage sludge, and wheat straw. Comparability between the three feeds was established by pre-treatment of sample size and moisture content. A detailed analysis was carried out including ultimate and proximate analyses. TGA experiments showed the distinctive devolatilisation behaviour of the feedstock. Solar-driven pyrolysis tests in pure argon atmosphere were performed and the evolving gases H_2, CO, CO_2 and CH_4 were measured at a test bench powered by a 7 kW_e solar simulator. Powder samples of 150 mg were irradiated from the top. Sewage sludge and wheat straw are more favourable for solar-driven pyrolysis than microalgae due to higher yields of product gas with higher ratios of H_2 and CO. Among the three feedstocks compared, wheat straw is the most favourable for solar-driven gasification, related with higher carbon conversion (78% for straw versus 38% for the sludge and 27% for the algae) and higher ratios of H_2 and CO. Later similar tests were also performed with microalgae "Chlorella Vulgaris", which was processed at several institutes (Fig. 5). Steam gasification tests were also performed resulting in higher syngas yields [7].

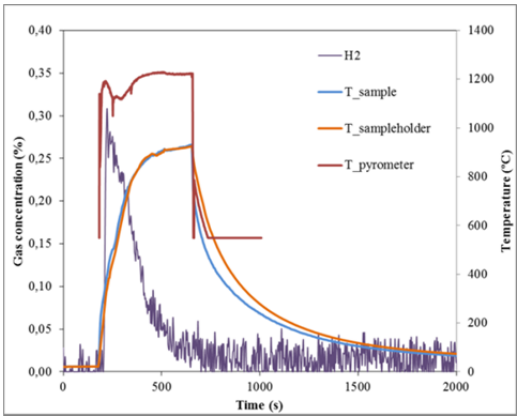

Figure 5. Temperatures and hydrogen concentration as a function of time during solar-driven pyrolysis of microalgae "Chlorella Vulgaris".

- Solar flash pyrolysis tests of biomass

CNRS performed in-depth studies of solar pyrolysis of beech wood with the objective of determining the optimal pyrolysis parameters for maximizing the lower heating values (LHV) of the gaseous products because they can be further utilized as fuel gas for power generation, heat production, and conversion to liquid transportable fuels. Fig. 6 shows the equipment. The total gas LHV strongly increases with increasing temperature (from 600 to 1200°C) and increasing heating rate (from 5 to 50°C/s), which is mainly due to increases in the CO and H_2 yields [8]. The LHVs (lower heating values) for gas, char and oil were determined from empirical equations. The gas product yield and LHV significantly increase with temperature (Fig. 7), which is mainly due to more H_2 and CO formation by enhanced secondary tar reactions. The char and oil characteristics highly depend on the temperature. Their high

energy contents show that the obtained char and oil can be utilized as valuable solid and liquid fuels. The biomass energy upgrading due to solar processing ranges from about 25% to 53% accounting for the uncertainty of bio-oil water content [8].

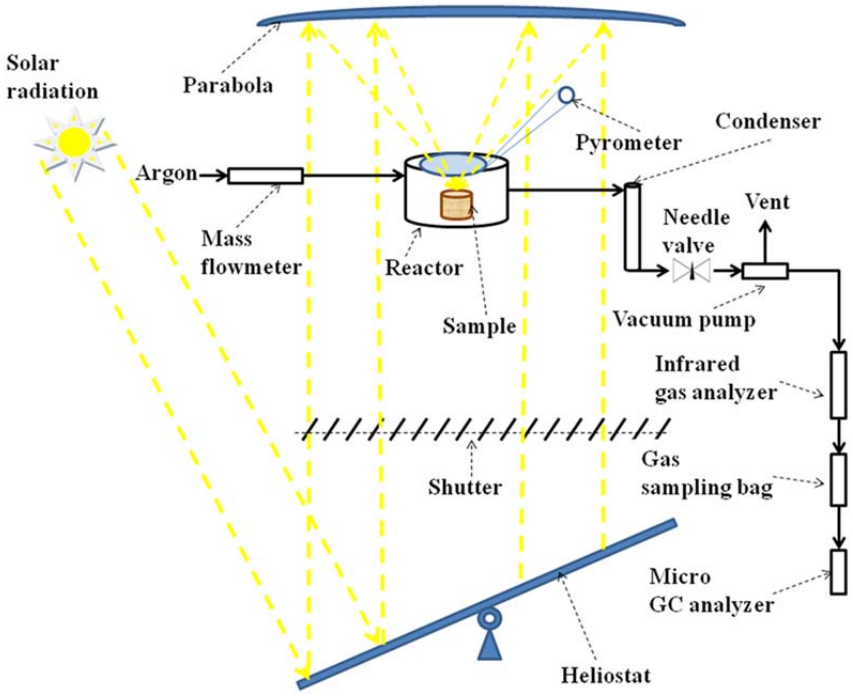

Figure 6. Scheme of the test installation for biomass pyrolysis at CNRS ("Controlled atmosphere crucible reactor" heated from the top).

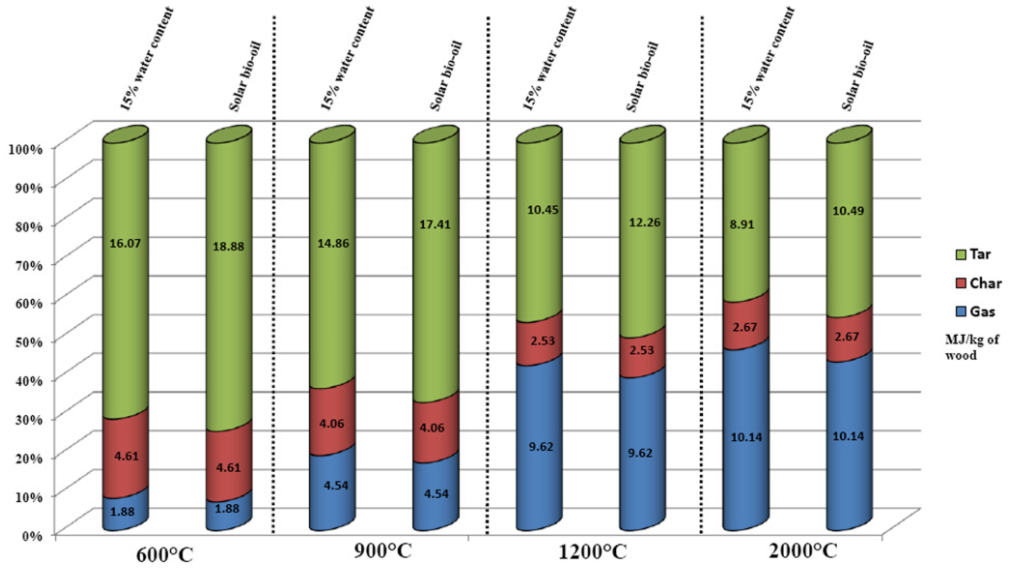

Figure 7. Graphic example of bar chart. Distribution of product energy content as a function of temperature for two water contents in the tar.

In the last year CNRS performed a similar investigation for pine sawdust and microalgae in the same crucible reactor varying pellet size, heating rate and final reactor temperature. The highest gas yield of more than 55% was found for the smallest pellet size (5mm), the highest final reactor temperature (1600°C) and the highest heating rate (50°/min) tested.

2.4 Novel solar reactor concepts

- Solar gasification in a gas-solid trickle-bed reactor

The performance of a gas-solid trickle-bed reactor including a high thermal conductivity porous ceramic packing from SiSiC has been investigated (Fig. 8) [3]. Beech char particles were used as the model feedstock. A series of 43–51 min gasification experiments in the temperature range 1173–1273 K with a mass flux of 6.5 g/s m^2 was conducted with no pressure increase or clogging over the duration of the experiments. Compared to the drop-tube configuration, the carbon conversions attained under same conditions in the trickle-bed were significantly higher (<1% vs. 52%, Fig. 8).

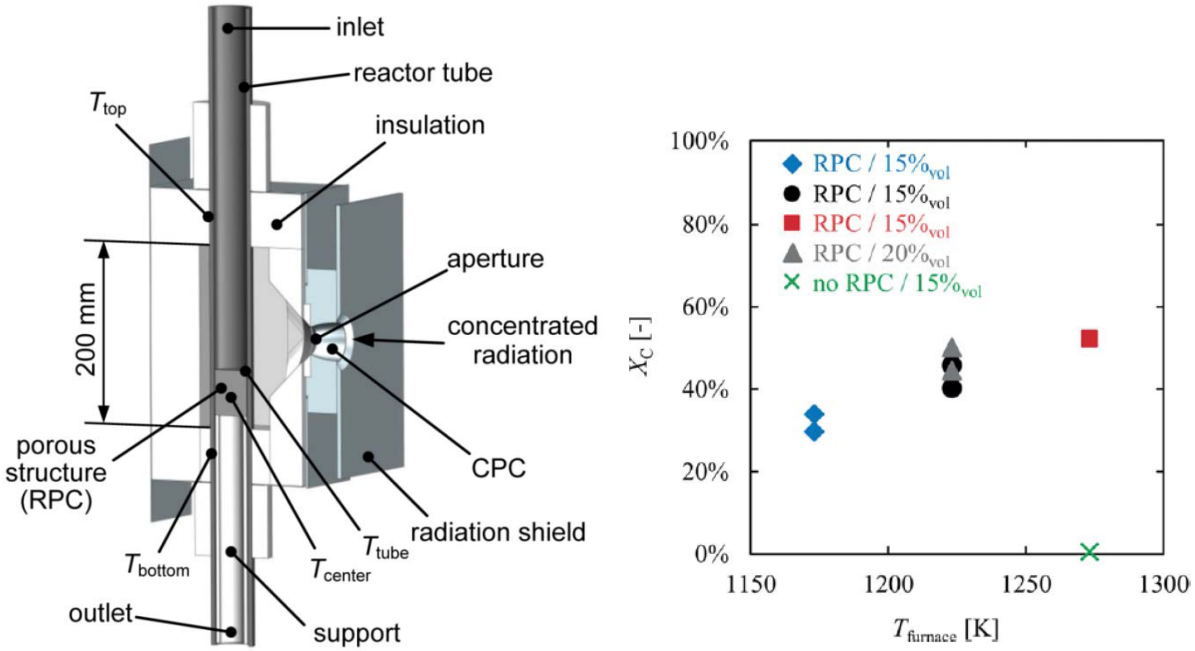

Figure 8. Left: Schematics of the trickle bed reactor at ETHZ. Right: Carbon conversion as a function of temperature with and without the SiC-RPC [3].

- Pressured vortex flow reactor

ETHZ with participation of PSI developed and demonstrated windowless indirectly irradiated pressurized and windowed directly heated atmospheric vortex flow gasification reactors (Fig. 9). Charcoal slurry has been gasified in a high flux solar simulator at ETHZ at pressures up to 6 bar. A peak solar-to-fuel energy conversion efficiency of 20% and almost complete conversion in less than 5 s point out to the technical feasibility of the solar reactor technology. For all 51 indirectly heated solar runs, the calorific value of the feedstock was upgraded in the range 16–35% [9]. High-quality pressurized syngas with no tars was produced, facilitating its integration to gas-to-liquid processing. In some tests Ar was substituted by CO_2, increasing the partial pressure of the gasifying agent and eliminating the consumption of expensive inert gas. Higher reaction extents and comparable solar-to-fuel energy conversion efficiencies and calorific upgrade factors were obtained on average with the indirectly-irradiated solar reactor than with the directly-irradiated solar reactor.

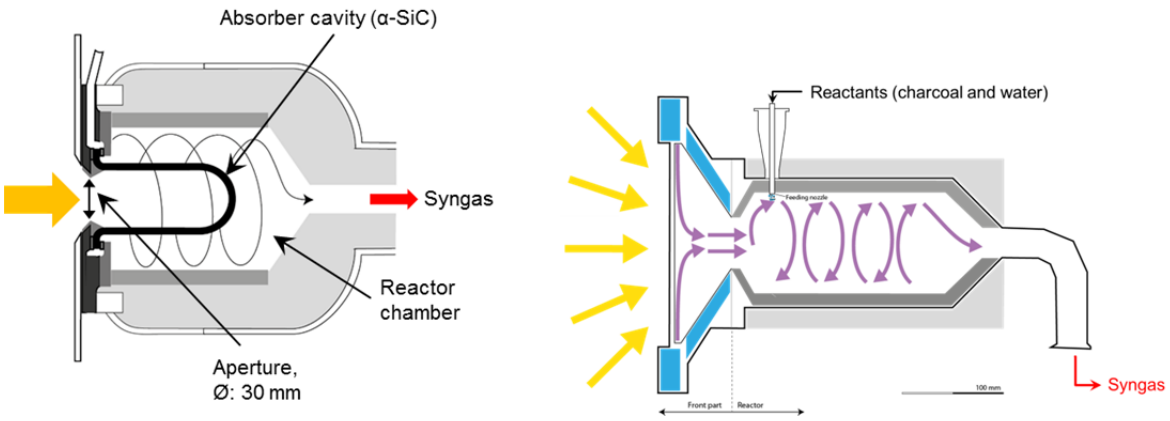

Figure 9. Scheme of the vortex flow reactor (a) indirectly heated (1-6 bar), (b) directly heated (1 bar due to flat window).

The major solar reactor concepts under study at the project partners have been described in the Deliverable 9.1. Tables 3 and 4 provide the overview tables from this Deliverable report, as issued in January 2017. Meanwhile in January 2018 scale-up versions of two reactor types listed in Table 4 reached the start-up phase:

- Section 3.9: Scale-up to 50 kW_{th} (TRL 5) at IMDEA (project SUN to LIQUID)
- Section 3.11: Scale-up to 750 kW_{th} (TRL 6) at PSA (project HYDROSOL PLANT).

Section	Reactor type	Main application(s) so far	Temperature range (°C)	Pressure range	Reactor size(s), concentrated radiation power input	TRL	Remarks
2.1	Packed bed two-cavity reactor (PSI)	(i) Carbothermal reduction of ZnO (Solzinc); (ii) Thermal treatment of waelz oxide; (iii) Steam gasification of carbonaceous materials (Solsyn)	1,000 - 1,400	Ambient	5 kW (lab); 150 kW (pilot Solsyn at CIEMAT-PSA), 300 kW (pilot Solzinc)	5	Thermal efficiency up to about 30% Up to 50kg/h Zn-dust production Solar upgrade up to 30% (LHV of produced syngas versus LHV of converted feedstock)
2.2	Packed bed cavity reactor (ENEA)	Hydrogen production using thermochemical cycle based on Na-Mn mixed ferrites	750 - 800	1 bar	1 kW (solar power concentr. in the cavity)	3 - 4	
2.3	Graphite tubes pilot scale solar reactor (CNRS)	Thermal decomposition of methane and natural gas	1,335 - 1,655	1 bar	50 kW	4 - 5	Solar upgrade of 8% of the high heating value of the products
2.4	Gas-solid trickle-bed reactor (ETHZ)	Biomass gasification	900 - 1,000	Ambient	1-3 kW (lab)	3 - 4	Carbon conversion up to 52%
2.5	Falling particle vacuum reactor (PSI)	Carbothermal reduction of ZnO	1,300 - 1,700	1 - 1,000 mbar	5 kW	3 - 4	
2.6	Pressurized vortex flow solar reactor (ETHZ)	Steam gasification of charcoal powder	1,000 - 1,300	1 - 6 bar	3 kW, 3,700 suns (lab)	4	Carbon conversion up to 94%, Solar-to-fuel energy conversion efficiency up to 20%
2.7	Shell-and-tube membrane reactor heated with molten salts (ENEA)	Steam methane reforming	450 - 550	9.5 bar	2 Nm^3/h H_2 - 10 kW_{th}	5	
2.8	Molten salts heated reactor for hydro-thermal liquefaction (UNIPA/ENEA)	Hydrothermal liquefaction and gasification of biomass and model compounds	200 - 550	Ambient - 300 bar	tubular reactor volume: 10 mL. Heating: 3.5 kW (lab)	2 - 3	Continuous high pressure (260 bar) process carried out. Upgrade to TRL 4 expected in next 1-2 years

Table 3. Overview about reactor types described in D9.1 (part 1). "Section" refers to the chapter in D9.1.

Section	Reactor type	Main application(s) so far	Temperature range (°C)	Pressure range	Reactor size(s), input concentr. radiation power	TRL	Remarks
3.1	Directly heated rotary reactor (PSI)	Thermal dissociation of ZnO	1,600 - 2,000	Ambient	10 kW (lab); 100 kW (pilot)	4 - 5	ZnO dissociation rates up to 28 g/min totalling over 28 kg during 13 full days of pilot experimentation
3.2	Solarized rotary kiln (IMDEA)	Reduction of non-volatile metal oxides	700 - 1,300	Ambient	1 kW	3	Only for lab-scale experiments for determination of materials abrasion and mechanical strength
3.3	Reduced pressure rotary solar reactor (CNRS)	Reduction of ZnO and SnO2 powders	up to 1,600	180 - 850 mbar	1 kW	3	Max. dissociation yield: 87% (Zn weight content in the final powder) with a typical dilution ratio of 300.
3.4	Gas-particle vortex flow reactor (CIEMAT, ETHZ)	Production of syngas from heavy crude oil	825 - 1,075	2 bar	5 kW (ETHZ/PSI); 500 kW (CIEMAT-PSA)	4	Chemical conversion for steam and petcoke after a single pass reached up to 35% (500 kW reactor)
3.5	Directly irradiated fluidized bed reactor (CIEMAT/IMDEA)	Hydrogen production by thermochemical cycles	800 - 1,000	Ambient	1 kW	3	Only for lab-scale experiments
3.6	Directly irradiated packed bed reactor (IMDEA)	(i) Kinetics determination of gas-solid reactions under high-radiation fluxes; (ii) Solar gasification and solar	Ambient - 1,800	Ambient + 300 mbar	1 kW	3	Only for lab-scale experiments on determination of chemical kinetics
3.7	Upward moving bed solar reactor (CNRS)	Reduction of ZnO and SnO2 powders	up to 1,600	180 mbar	1 kW	3	Only for lab-scale experiments
3.8	Controlled atmosphere crucible solar reactor (CNRS)	Solar pyrolysis of biomass	600 - 2,000	0.44 - 1.14 bar	1.5 kW	3	A maximum gas production of 62% with a LHV of 10,376 ± 218 (kJ/kg of wood) (1,200 °C, 50 °C/s, 0.85 bar and 12 NL/min)
3.9	Cavity reactor for Ceria (ETHZ)	Splitting of CO2 and H2O	700-1,600	ambient	2.8-3.8 kW, 3000 suns (lab)	4	Solar-to-fuel energy conversion efficiency up to 1.72 % (without sensible heat recovery). Scale-up under realization
3.10	Pressurized volumetric receiver (DLR)	Solar Steam Reforming of Methane Rich Gas	up to 900	15 bars	400 kW	5	CH4 conversion 94.6%
3.11	Monolithic honeycomb reactor (Hydrosol) (DLR)	Splitting of H2O	800 -1,300	ambient	< 10 kW Solar furnace, 100 kW Tower, 750 kW Tower in constr.	5	Upgrade to TRL 6 expected in 750 kW plant under construction

Table 4. Overview about reactor types described in D9.1 (part 2). "Section" refers to the chapter in D9.1.

2.5 Novel processes for solar fuel production

- <u>(Near) critical water gasification and liquefaction of biomass</u>

Two novel processes have been investigated: (a) super-critical water gasification (SCWG) and near-critical water gasification and/or liquefaction (NCWG/L) of biomass for the production of syngas and liquid bio-fuels, by ENEA and UNIPA.

ENEA studied supercritical water gasification (SCWG) processes that can be potentially heated with molten salt streams from CST plants. Gasification of two different types of biomass was considered in this activity: (i) digestate of agricultural and livestock sewage and (ii) microalgae. Gasification tests were carried out at 250 bar and 550°C in a lab-scale tubular reactor (Fig. 10). Tests carried out with digestate as feed attained gas yields of about 13% with a gas heating value of 22 MJ/kg of organic matter; hydrogen content of the gas was in the range 40-45 vol%, while methane content was about 15 vol%. As for the gasification of microalgae, the gas yield was strongly affected by the total solid content and values ranging from 10 to 30% were measured. In both cases, the residual liquid phases produced in the process contained organic compounds with a possible economic value for the chemical industry.

Figure 10. Facility for biomass gasification at ENEA Trisaia laboratory

Hydrothermal gasification and liquefaction tests at UNIPA with microalgae in *batch* reactors with and without catalysts were extended up to the first half of the third project year, in order to increase the number of catalysts tested in the hydrothermal liquefaction of commercial microalgae (Nannochloropsis gaditana). TiO_2-supported catalysts and Al_2O_3-supported catalysts were characterized in the HTL process (publication under preparation). Characterization of the obtained bio-oil was performed by LNEG (CHNS elemental analysis) and ENEA (GC-MS analysis), which analyzed 54 samples for a qualitative determination of the biocrude composition.

During the 4th year UNIPA studied the hydrothermal liquefaction of microalga Chlorella vulgaris supplied by LNEG as common biomass to the STAGE-STE partners. The research was carried out in cooperation with ENEA and LNEG. At UNIPA the effects of reaction time, temperature, and catalyst loading on the biocrude yield were studied in its batch reactor (Fig. 11) working at 300-400°C for 15-30 min with $CoMo/Al_2O_3$ and $NiMo/Al_2O_3$ catalysts [10]. LNEG, in order to compare the results of HTL with UNIPA, studied the effects of reaction time and temperature on process total conversion, product yields and product composition and performed tests with this feedstock for hydrothermal liquefaction in its small batch reactor (volume: 0.16 dm^3; height 5 cm). Similar sampling and analysis procedure were performed by both partners (this was the scope of a staff exchange from LNEG to UNIPA). The product quality was analyzed by LNEG (CHNS) and ENEA (GC-MS analysis).

ENEA and UNIPA furthermore performed a conceptual study of the coupling of a continuous plant for HTL of microalgae with a CSP plant using molten salts as heat transfer fluid, also providing input for Task 9.4. From the techno-economic analysis a minimum fuel selling price of the produced bio-oil of 2.19 USD/kg was estimated [11] (compare Chapter 5).

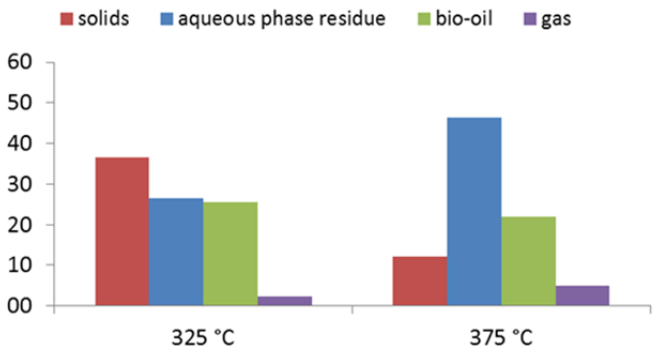

Figure 11. Results of batch tests at UNIPA with "joint" microalgae Chlorella Vulgaris for heat-up to different temperatures.

- Low temperature solar steam reforming

ENEA completed the construction of a pilot plant for hydrogen production by steam reforming of carbonaceous feedstocks with a capacity of 2 Nm^2/h of H_2 [12]. The plant includes a molten-salt heated membrane reactor coupled with a molten salt loop, which simulates a solar field by electrically heating the molten salt stream. An experimental campaign was conducted on the pilot plant including a total operating time of 150 h on stream and several start-up/shut-down procedures. Different combinations of operating conditions were tested: molten salt temperatures in the range 420-550°C; reaction side pressure 9.5 bar; steam-to-carbon ratios in the feed from 3 to 12; operation with or without sweep steam in the permeate space. Only methane was used as carbonaceous feed during the campaign, even if tests carried out in laboratory-scale integrated membrane reformers showed that the same catalyst-membrane combination used in the pilot can successfully process biogas and bioethanol streams. A methane conversion of about 60% was obtained at the nominal operating conditions of the plant (the maximum conversion for a conventional reformer under the same conditions is about 27%). The performance of the system remained stable during the whole experimental campaign, so that significant deactivation can be excluded for both the catalyst and membrane used in the reactor (Fig. 12).

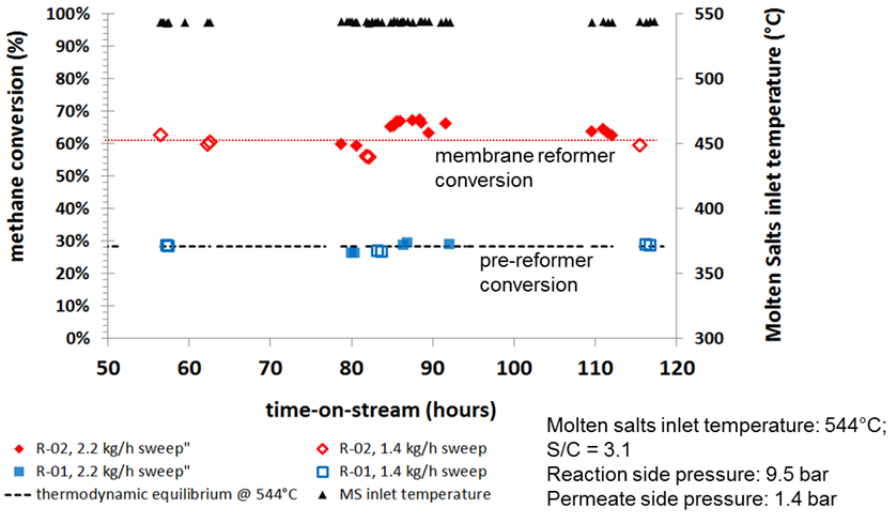

Figure 12. Conversion obtained in steam reforming pilot plant during operation at nominal conditions (ENEA).

2.6 Syngas purification and processing

This work is also relevant for syngas produced in thermochemical cycles (Chapter 3 resp. Task 9.2).

LNEG studied the purification options for further processing syngas of variable quality and possible additional conversion steps as well as potential uses [13, 14]. The Gasification of feedstocks containing nitrogen and sulphur promoted the partial conversion of these elements into pollutants like H_2S and NH_3. The acceptable contents of tar, H_2S and NH_3 in syngas depend on the gas application. The use in turbines, fuel cells and chemical synthesis require very low contents of these components. By the right selection of gasification experimental conditions, including the use of low cost mineral like, limestone, dolomite or olivine it is possible to control the release of tar, H_2S and NH_3. Calcium, magnesium and iron oxides present in dolomite or olivine may react with H_2S to form metal sulphides, which are generally retained inside the gasifier. In dolomite reactor there was a decrease in hydrocarbons and in CO contents, while CO_2 and H_2 concentrations increased. The same tendencies were also observed in the Ni-based reactor. For more demanding applications (turbines, fuel cells and chemical synthesis) it is advisable to treat gasification gas in a hot gas conditioning system to further decrease the contents of these compounds and also to favour the reforming of heavier gaseous hydrocarbons and tar to hydrogen and CO. A hot gas conditioning system was designed, built and tested. A reactor with two sequential fixed bed steps was used. In the first step a low cost catalyst, limestone, was used. The same catalyst may be used in the second step, but when a nickel based catalyst is used in the second step much lower H_2S and NH_3 contents are found and no tar was detected in syngas. The latter option further promoted cracking and reforming reactions and the conversion of hydrocarbons into CO and H_2. Water gas shift reaction was also favoured and thus the conversion of CO into H_2 and CO_2. The use of higher temperatures favoured all these reactions.

2.7 References for Chapter 2

1. A. Vidal, T. Denk, A. Steinfeld, L. Zacarías: Upscaling of a 500 kW solar gasification plant, 18th World Hydrogen Energy Conference 2010 - WHEC 2010, Parallel Sessions Book 3: Hydrogen Production Technologies - Part 2; Proceedings of the WHEC, May 16-21, 2010, Essen (Germany), Schriften des Forschungszentrums Jülich / Energy & Environment, Vol. 78-3, ISBN: 978-3-89336-653-8.
2. M.I. Roldan, J. Fernandez Reche, L. Valenzuela, A. Vidal, E. Zarza: CFD modelling in solar thermal engineering, engineering applications of computational fluid dynamics, Publisher: International Energy and Environment Foundation (Editor: Maher A.R. Sadiq Al-Baghdadi), Volume 3, Chapter 2, 47-84, 2015. ISBN 13: 978-1-51178-878-6.
3. M. Kruesi, Z.R. Jovanovic, A. Haselbacher, A. Steinfeld: Analysis of solar-driven gasification of biochar trickling through an interconnected porous structure, AIChE Journal **61**, 867-879, 2015. DOI:10.1002/aic.14672

4. C. Wieckert, A. Obrist, P. von Zedtwitz, G. Maag, A. Steinfeld: Syngas production by thermochemical gasification of carbonaceous waste materials in a 150 kWth packed-bed solar reactor, Energy & Fuels **27**, 4770-4776, 2013. DOI:10.1021/ef4008399

5. F. Müller, H. Patel, D. Blumenthal, P. Pozivil, P. Das, C. Wieckert, P. Maiti, S. Maiti, A. Steinfeld: Co-production of syngas and potassium-based fertilizer by solar-driven thermochemical conversion of crop residues, Fuel Processing Technology **171**, 89-99, 2018. DOI:10.1016/j.fuproc.2017.08.006.

6. M. Romero, C. Löhrl, J. Gonzalez-Aguilar, C. González-Fernández, M. Kaltschmitt: Solar-driven pyrolysis and gasification of low-grade carbonaceous materials. Proc. Hypothesis XI (HYdrogen POwer THeoretical and Engineering Solutions International Symposium) 2015, Toledo, Spain, 6 – 9 September 2015, 55ff. Edited by Servicio de Publicaciones de la Universidad Rey Juan Carlos, Madrid, Spain. ISBN: 978-84-697-0417-2.

7. L. Arribas, N. Arconada, C. González-Fernández, C. Löhrl, J. González-Aguilar, M. Kaltschmitt, M. Romero: Solar-driven pyrolysis and gasification of low-grade carbonaceous materials, Int. J. Hydrogen Energy **42**(19), 13598-13606, 2017. DOI:10.1016/j.ijhydene.2017.02.026

8. K. Zeng, D. Gauthier, R. Li, G. Flamant: Solar pyrolysis of beech wood: Effect of pyrolysis parameters on products distribution and gas products composition, Energy **93**, 1648, 2015. DOI:10.1016/j.energy.2015.10.008

9. F. Müller, P. Pozivil, P. van Eyk, A. Villarrazo, P. Haueter, C. Wieckert, G. J. Nathan, A. Steinfeld: A pressurized high-flux solar reactor for the efficient thermochemical gasification of carbonaceous feedstock, Fuel **193**, 432-443, 2017. DOI:0.1016/j.fuel.2016.12.036

10. R. Bleta, B. Schiavo, N. Corsaro, P. Costa, A. Giaconia, L. Interrante, E. Monflier, G. Pipitone, A. Ponchel, S. Sau, O. Scialdone, S. Tilloy, A. Galia: Cyclodextrin-assisted synthesis of mesoporous CoMo/γ-Al2O3 catalysts for the hydrothermal liquefaction of microalgae: toward more robust heterogeneous catalysts, submitted to ACS Applied Materials & Interfaces, currently (1/2018) under review.

11. A. Giaconia, G. Caputo, A. Ienna, D. Mazzei, B. Schiavo, O. Scialdone, A. Galia: Biorefinery process for hydrothermal liquefaction of microalgae powered by a concentrating solar plant: a conceptual study, Applied Energy **208**, 1139–1149, 2017. DOI:10.1016/j.apenergy.2017.09.038

12. A. Giaconia: Multi-fueled solar steam reforming for pure hydrogen production using solar salts as heat transfer fluid. Energy Procedia **69**, 1750-1758, 2015.

13. F. Pinto, R. André, C. Carolino, M. Miranda: Hot treatment and upgrading of syngas obtained by co-gasification of coal and wastes, Fuel Processing Technology **126**, 19–29, 2014. DOI:10.1016/j.fuproc.2014.04.016.

14. F. Pinto, R. André, M. Miranda, D. Neves, F. Varela, J. Santos: Effect of gasification agent on co-gasification of rice production wastes mixtures, Fuel **180**, 407–416, 2016. DOI:10.1016/j.fuel.2016.04.048.

3. Task 9.2 "Solar fuels from thermochemical cycles"

In this task led by PSI with further participants CIEMAT, DLR, CNRS, ENEA, ETHZ, IMDEA and ASNT long-term solar fuel production technologies for H_2 and syngas production have been studied and innovative solar chemical reactor concepts were experimentally tested at laboratory scale (1-10 kW_{th}) and pilot scale (100 kW_{th}). For the most advanced processes, input to economic analyses of industrial plants has been generated based on test results and validated reactor models. These analyses have been conducted in Task 9.4 and are reported in Chapter 5.

3.1 Reactor and process modelling

Related to major research activities described in subchapters 3.2, 3.3 and 3.4 numerous modelling activities have been performed with a varying degree of sophistication. Significant respective investigations include the following:

- Modelling for thermal dissociation of ZnO in a directly irradiated rotary reactor (Chap. 3.2)
At PSI, a non-linear dynamic model has been developed and applied to this solar reactor for ZnO dissociation under ambient pressure conditions [1]. The model includes 3D governing unsteady mass and energy conservation equations, combined radiation-conduction-convection heat transfer coupled to reaction kinetics, and radiative exchange within absorbing-emitting-scattering particle bed undergoing thermochemical transformation. Monte Carlo ray-tracing technique and radiosity enclosure theory are employed to resolve the radiative exchange within the solar cavity receiver and the semi-transparent spectrally-selective quartz window. The model has been validated by comparing predicted temperatures and reaction extents with experimental data obtained from a 10 kW_{th} solar reactor prototype [2] and from the 100 kW_{th} solar pilot reactor (see Chapter 3.2).

- Modelling of carbothermal reduction of ZnO in the falling particle vacuum reactor (Chap. 3.3)
At PSI a steady state reactor model based on Monte Carlo ray tracing for the incoming radiation from PSI's High Flux Solar Simulator and accounting for spectral and directional optical properties and temperature dependent chemical kinetics was developed and successfully validated with the experimental data [3].

- Modelling of carbothermal reduction of ZnO in a packed bed reactor (for reactor see Chap. 2.2 and 4.1).
At ETHZ/PSI dynamic modelling of the packed bed solar reactor used for different applications has been performed for carbothermal reduction of ZnO [4]. The work included a study of the effect of a semi-continuous feeding (periodic introduction of new feedstock batches e.g. in a pusher type solar reactor (Fig. 13). For the studied lab-scale case this resulted in an increase of the solar to chemical conversion efficiency from 15.5 to 16.9%, this at a 22% higher averaged Zn-production rate.

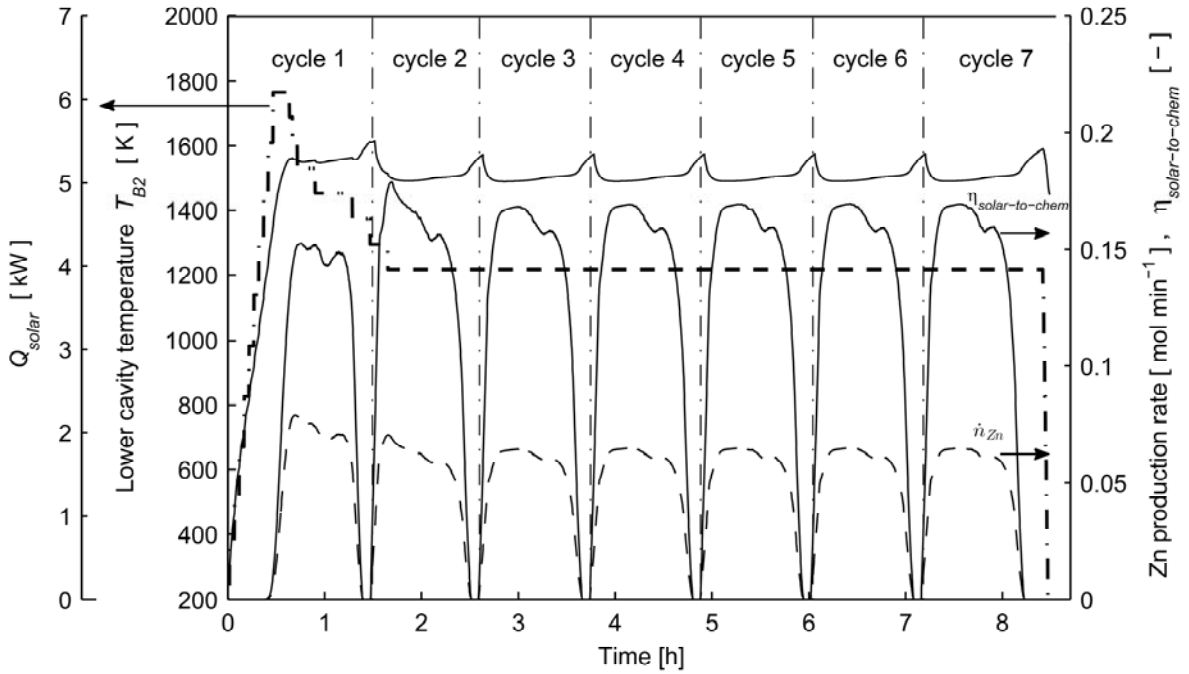

Figure 13. Temporal variation of the solar radiative power input, LC temperature, Zn(g) production rate, and solar-to-chemical energy conversion efficiency for semi-continuously feeding of seven 35 mm-high packed beds of ZnO and beech charcoal into a 10 kW_{th} packed-bed solar reactor [4].

3.2 Solar pilot plant for ZnO dissociation

Continuous stable operation of PSI's 100 kW_{th} solar pilot plant for the thermal dissociation of ZnO in a directly irradiated rotary reactor (Fig. 14) has been demonstrated above 2000 K during two extended experimental campaigns at the High-Flux Solar Simulator at PSI and at the Megawatt Solar Furnace of CNRS in Odeillo. In the first campaign at PSI in-situ flow-visualization experiments were conducted at 1600 K in order to prevent particle-laden fluid flows near the window from attenuating transparency by blocking incoming radiation. It was shown that high-temperature in-situ flow visualization is possible by use of CO-pulsing inside the cavity of a solar thermochemical receiver-reactor, thereby allowing for accurate assessment and optimization of aerodynamic window protection [5] In the second campaign at CNRS solar power delivered to the reaction cavity ranged between 90 and 128 kW_{th}, at peak solar concentration ratios as high as 4,671 suns. The products Zn and O_2 were quenched with Ar(g) and recovered in a filter battery, where collected particles contained molar Zn-content as high as 44 %. During experimentation, switching between product collection filter cartridges resulted in 54 unique experiments, where a maximum solar-to-chemical efficiency of 3 % was recorded for the solar reactor. The project has been successfully completed and the main research results have been published [6-7].

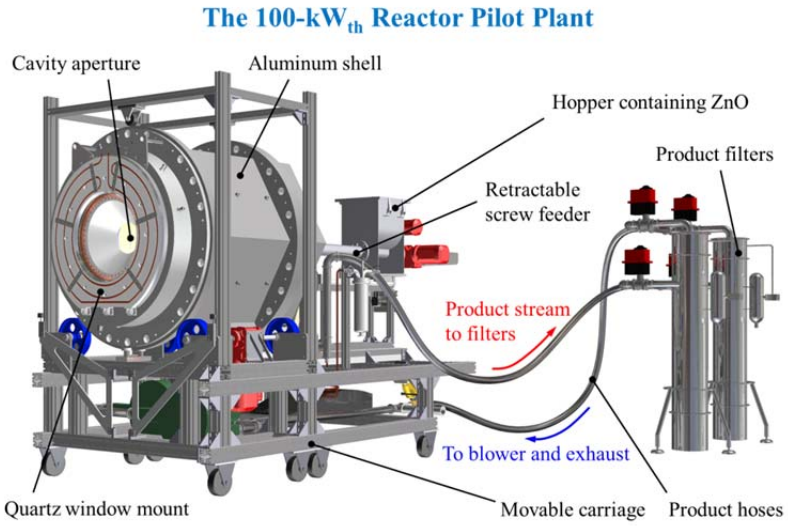

Figure 14. ZnO pilot plant layout utilized in experiments conducted at PSI and Odeillo in 2014.

3.3 Novel solar reactor concepts

A survey of the solar reactor concepts available at the STAGE-STE WP9 partners including their development status (TRL-level) and their main applications related to Tasks 9.1 and 9.2 is provided in Deliverable 9.1. Tables 3 and 4 in Chapter 2.4 show overview tables from D9.1.

In the following four some respective activities are highlighted, which were specifically performed within STAGE-STE:

- Directly irradiated packed bed reactor

IMDEA has designed and assembled a laboratory test bed using a "beam-down" type chemical reactor for the analysis of the reducing step of non-volatile metal oxides, such as cerium oxide. The system is powered with a 7 kW_e Xe-arc lamp located at one of the foci of an ellipsoidal mirror providing a radiant power above 1 kW_{th}. The concentrated beam is re-directed downwards by a water-cooled mirror tilted 45 degree. The vertical axis reactor contains a crucible-type sample holder to accommodate the ceria powder. The dimensions of the reactor and sample, gas flow rate and focusing strategy were optimized with COMSOL to achieve the temperature required by the reaction. The beam-down tests with ceria have been completed [8].

- Solarized rotary cavity reactor

IMDEA has commissioned and characterized a 1 kW_{th} directly-irradiated solar rotary cavity reactor used for thermochemical reactions of manganese oxide (Fig. 15). Pellet samples were directly irradiated by concentrated radiation provided by a 7 kW_e high-flux solar simulator (HFSS). The rotating cavity was promoting good mass and heat transfer, as well as high surface area for the reactions. Optical simulations and CFD analyses showed that 1 kW of incident power and 1700 K can be reached in the reaction zone, which is located at the

secondary focus of the HFSS. The test results have been presented at the Solar World Congress 2015, Daegu, Korea [9].

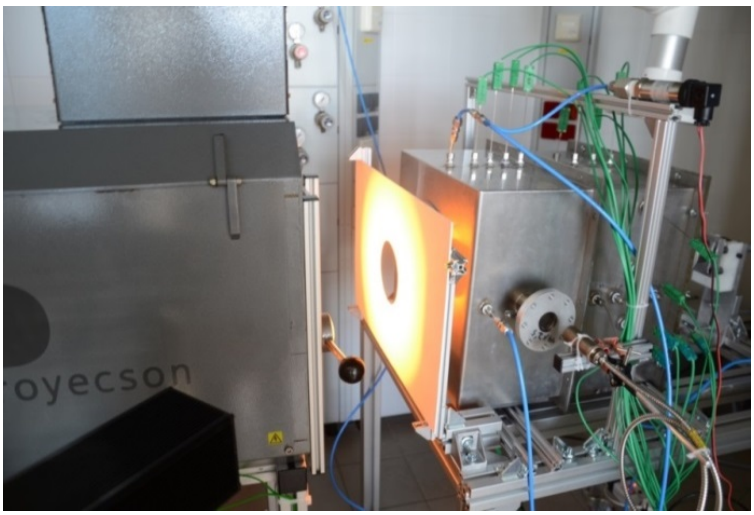

Figure 15. Experimental setup showing rotary kiln in front of high-flux solar simulator (IMDEA).

- Directly irradiated fluidized bed reactor

In a joint activity between IMDEA and CIEMAT a 1 kW_{th} fluidized bed reactor developed by CIEMAT was adapted and installed in the 7 kW_e high flux solar simulator at IMDEA. The experimental test bed required the installation of a water-cooled mirror in order to modify the direction of the light beam from horizontal to vertical directions. After general performance tests of the reactor with inert particles (SiC) various assays were conducted using commercial nickel ferrite particles (pre-treated for the required particle size distribution). Maximum temperature achieved was between 850 and 900 °C, insufficient for the reduction reaction. Therefore a new tailor-made directly irradiated fluidized bed reactor was designed and realised for this radiation source (Fig.16). It has been commissioned in 2017 at IMDEA. After preliminary cold tests with SiC pellets, first hot tests were performed with $NiFe_2O_4$ and CeO_2. E.g. for $NiFe_2O_4$ pellets of $d_p > 100$ µm fluidization could be achieved during the test for a flowrate of 6 l/min, while temperatures above 1000ºC were measured. Follow up research is trying to reduce sintering also observed in these first tests by introduction of inert and/or structural substrate material.

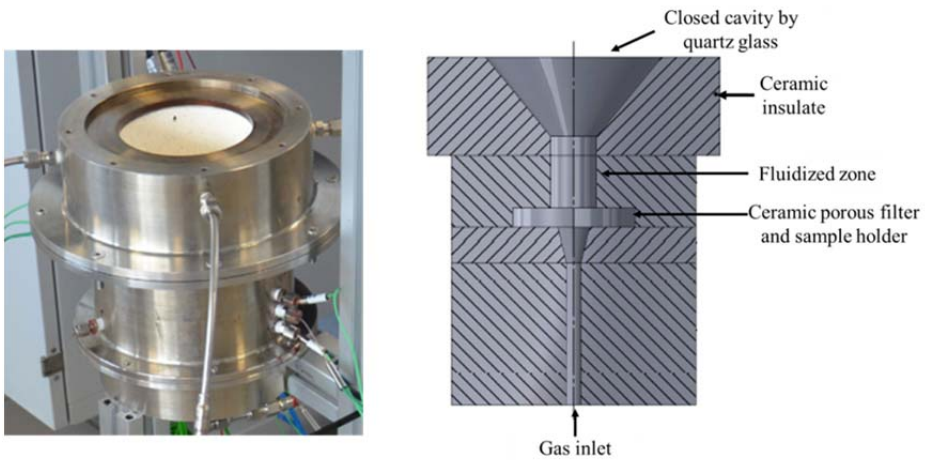

Figure 16. 1 kW_{th} fluidized bed reactor installed at IMDEA. Left: External stainless-steel vessel; Right: Reactor layout

- Falling particle vacuum reactor

At PSI, a solar-driven aerosolized particle reactor under vacuum was tested for carbo-thermal reduction of ZnO using concentrated radiation from PSI's a high-flux solar simulator (Fig. 17). The reactor concept is based on the downward flow of ZnO and carbon particles, which are indirectly heated by an opaque intermediate absorption tube [10]. The particles are rapidly heated to reaction temperature and reduced within residence times of less than 1 s. In continuous feeding experiments, maximum sustained temperatures close to 2000 K and heating rates as fast as 1400 $Kmin^{-1}$ could be achieved for pressures between 1 and 1000 mbar (Fig. 18 shows a typical test). Reduction in system pressure leads to decreased particle residence time, and therefore low conversion, thus partially diminishing the positive thermodynamic effects of vacuum operation. Experimental results highlight the necessity of balancing the system design in order to optimize the conflicting influence of vacuum operation and reacting particle residence time.

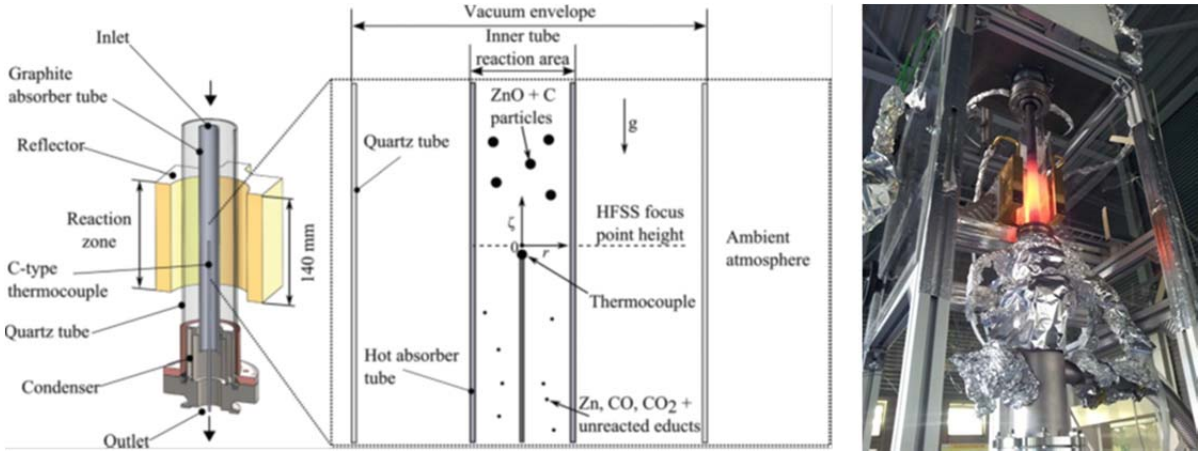

Figure 17. Left: Schematic of the vacuum aerosol reactor as a cross-sectional view, and an enlarged view of the graphite absorber tube showing the hot reaction zone and particle flow [10]. Right: Solar reactor prototype for ZnO dissociation under vacuum after experimentation at PSI's High-Flux Solar Simulator, showing after-glowing absorber tube.

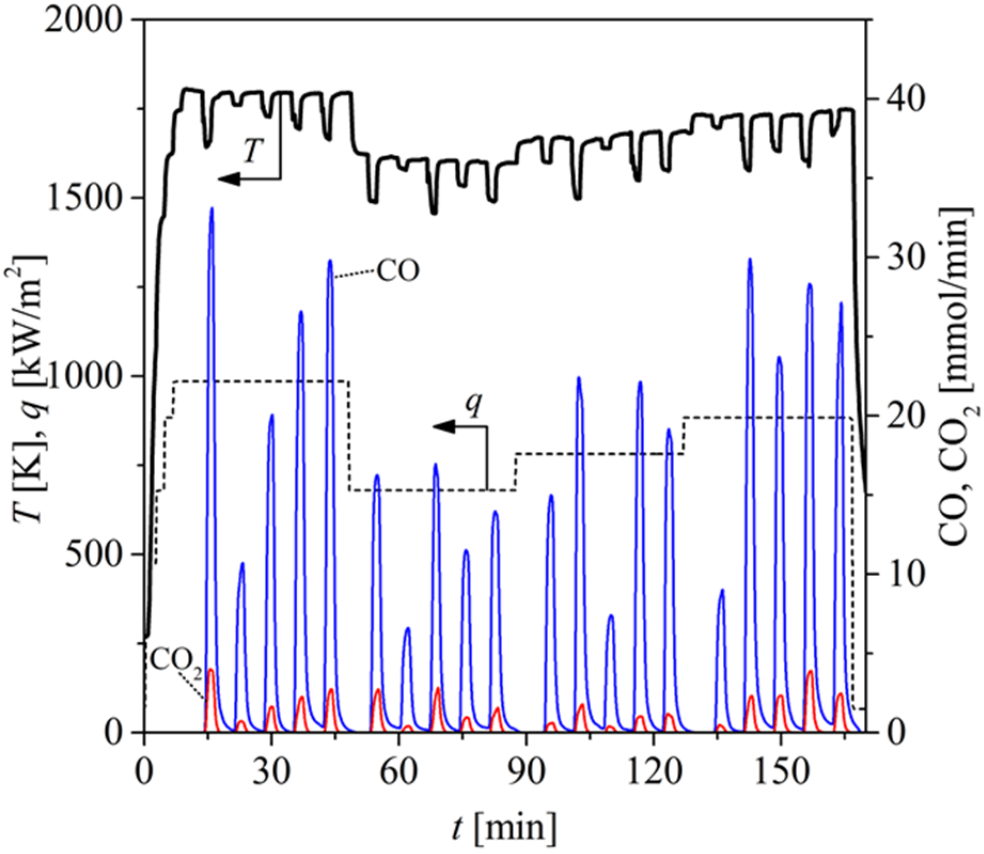

Figure 18. Measured temperature TC at the focal height of the HFSS and radiative flux q_{rad} (left axis) and molar flow rates of evolved gases (right axis) for a typical reaction capacity experiment at p = 100 mbar.

3.4 Novel processes for solar fuel production

Two processes (four-step photo chemical sulphur ammonium cycle and manganese ferrite with sodium carbonate) were specifically mentioned in the DoW to be investigated. During the course of the project we decided to also perform studies of perovskites and of the use of thermochemical cycles for O_2 separation from the product gas. Furthermore a screening study for thermochemical cycles was performed.

- Sulphur based thermochemical cycles

A study of ammonium sulphate decomposition has been completed with a modified sulphur ammonium cycle investigated in a national research program (PRIN 2009, “Optimization of the photothermocatalytic sulfur-ammonia process for hydrogen production”). The original sulphur ammonia process [11] was modified in order to reduce the material cost and/or the temperature of the step involving oxygen and sulfur dioxide production with the introduction of metal oxides (e.g. from Zn, Co or Ni) for the ammonium sulfate decomposition. This results in a four step cycle represented e.g. in the case of ZnO by the following simplified reactions:

(1) $(NH_4)_2SO_3 + H_2O \rightarrow (NH_4)_2SO_4 + H_2$ (photocatalytic, room temperature ~ 80°C)

(2) $ZnO + (NH_4)_2SO_4 \rightarrow ZnSO_4 + H_2O + 2NH_3$

(3) $ZnSO_4 \rightarrow ZnO + SO_2 + 1/2\ O_2$ (endothermic)

(4) $SO_2 + 2NH_3 + H_2O \rightarrow (NH_4)_2SO_3$

The highest temperature is required for reaction (3), which occurs at about 850°C. Also the use of iron (III) oxide was evaluated, obtaining the sulfate $Fe_2(SO_4)_3$ that decomposes below 700°C [12]. Advantages and drawbacks of the modified cycle were investigated, along with the conversion rates of the metal sulfates into SO_2. Overall, the results were promising but the photocatalytical step (1) remains too slow, leading to a large size of the hydrogen production reactor.

The focus of the further work was on the solar SO_3-decomposion which is relevant for all sulphur family thermochemical cycles as well as the hybrid sulphur cycles also being in focus. ENEA developed catalysts for the SO_3 decomposition step of the sulphur-family thermochemical cycles. Fe_2O_3-based catalysts were studied considering different ceramic supports including solid monolithic foams and granular materials (Fig. 19). Both the activity and stability (up to 50 h on stream) of the catalysts were studied. The SO_3 conversion data collected (1 bar, 800-900°C) were analysed with a kinetic model in order to obtain a reaction rate expression to be used in the design of a full-scale reactor.

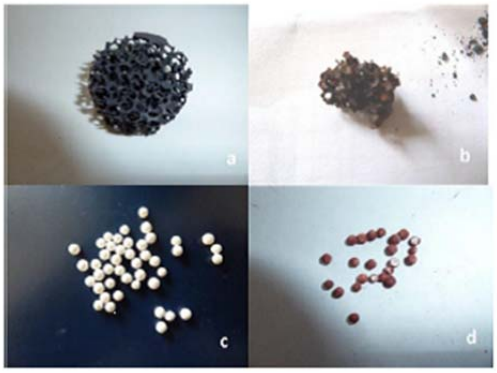

Figure 19. Bare and catalysed supports used for SO_3 decomposition: a) SiC foam (bare); b) SiC foam (catalysed); c) Al_2O_3 beads (bare); c) Al_2O_3 beads (catalysed). (ENEA)

<u>- Manganese ferrite cycle in presence of sodium carbonate</u>

An experimental study of reaction kinetics as well as development and on-sun testing of a 1 kW cavity reactor has been conducted.

The solar reactor developed is a horizontally oriented cylindrical open cavity receiver made of Inconel 625, which traps the focused incident radiation. The thermal energy is delivered to the reaction chamber by conduction through the metal cavity walls. The cylindrical receiving cavity (diameter 64 mm, height 83 mm) is surrounded by an annular space (internal diameter 72 mm, external diameter 102 mm) in which two flow distributors are inserted. A sketch of the reactor is shown in Fig. 20. Gases enter the reactor from a pipe positioned in the back-side

of the reactor (IN) and are conveyed in the annular cavity. The gas flow then splits and flows into the packed bed formed by pellets of the active material, where heat exchange and chemical reactions take place. The flow recombines at the outlet were effluent gases are collected through a second flow distributor, to an outlet pipe (OUT) and sent to gas analysis. More reactor details are provided in Deliverable 9.1, Section 2.2.

The packed-bed cavity reactor has been tested in a small solar concentration facility (about 1 kW) located on the roof of the Chemistry Department of the University "La Sapienza" of Rome.). The concentrated solar radiation is directed towards The reactor-receiver cavity is placed in the focus of the concentrating dish of a solar furnace.

The experimental campaign carried out on the reactor confirmed the feasibility of the process [13]. An efficiency slightly below 1% was calculated based on the experimental results, even if this value is not representative of the actual potential of the process, since the reactor capacity is very low and the reactor configuration and thermal insulation system still need to be optimized.

Furthermore, in order to support the design and scaleup of the solar reactor, an off-sun experimental campaign was carried out in a fixed-bed laboratory-scale reactor operating under controlled conditions [14]. The results of such campaign allowed to validate a simple shrinking-core model for the reaction kinetics.

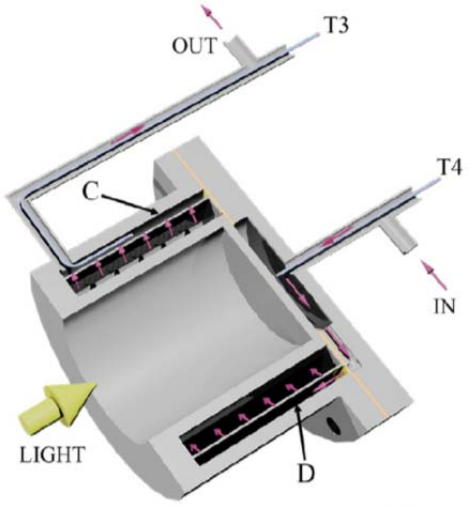

Figure 20. Scheme of the packed-bed cavity reactor for solar reduction of manganese ferrite in the presence of sodium carbonate.

- Perovskites-materials for thermochemical cycles

CIEMAT explored new perovskite materials such as $La_xSr_{1-x}Mn_yAl_{1-y}O_3$, $La_xSr_{1-x}Fe_yAl_{1-y}O_3$ (LSFA) and $La_{0.5}Sr_{0.5}CoO_3$ as candidates for thermochemical cycles. First test carried out in a thermogravimetric analyser with 4 cycles at 1150 ºC for activation and 950º C for hydrolysis indicate that in these materials the recovery of O_2 is complete for the operation conditions (Fig. 21).

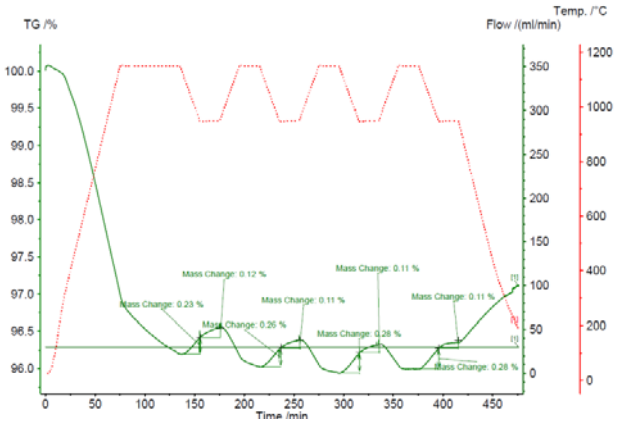

Figure 21. Thermogravimetric results for $La_xSr_{1-x}Fe_yAl_{1-y}O_3$ during 4 cycles

The next step involved the use of a tubular furnace coupled with a gas chromatograph (Varian CP4900) equipped with a molecular sieve column and a thermal conductivity detector, etc. (Fig. 22, left). First hydrolysis tests carried out indicated that (a) oxygen release in perovskite materials is higher than Nickel ferrites (Fig. 22, right). However hydrogen production is lower than the expected one according to the oxygen released in the reduction step. Furthermore, the oxygen released in the reduction step decreased in each consecutive cycle showing that cobalt perovskite is not a stable material.

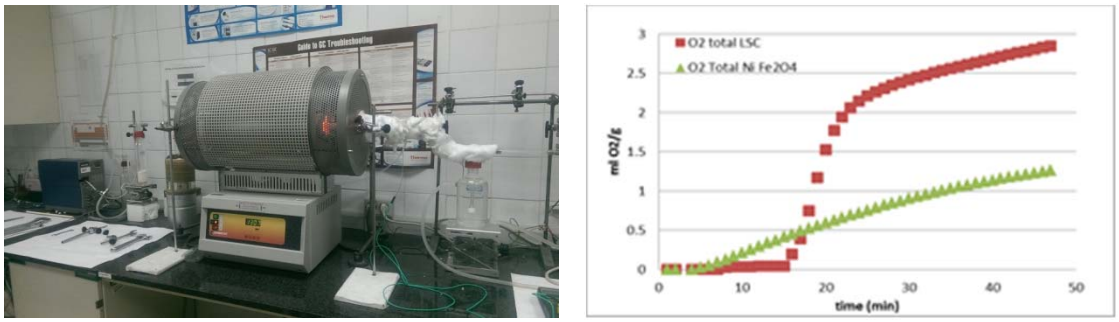

Figure 22. Left: Horizontal tubular furnace to evaluate thermochemical cycles; Right: Oxygen released on the regeneration step from $NiFe_2O_4$ and LSC samples.

<u>- O_2-separation</u>

PSI is investigating the separation of O_2 from gas mixtures resulting from the high-temperature solar thermochemical dissociation of metal oxides – such as ZnO. Since solar thermochemical cycles inherently suffer from heat losses, it would be beneficial to utilize an oxygen separation technology driven by low-grade process heat, i.e., solar-thermal waste heat, without penalizing the solar-to-fuel energy conversion efficiency. Thermochemical O_2 separation using perovskite redox materials enable low operating temperatures and the possibility to produce high-purity inert gas. This research project proposes to utilize a dual approach to the rational design of perovskite redox materials by combining computational materials science and experimental characterization methods [15].

- Screening of TC materials

ASNT has performed a screening of the different TC cycles analysed for the production of H_2 and CO, classifying the cycles in CO_2/CO systems, H_2/H_2O systems, carbonation reactions, perovskite structures, hercynite cycles, and others (Fig. 23). The screening mainly covers temperatures of reaction, heats of reaction and main advantages/disadvantages of each cycle.

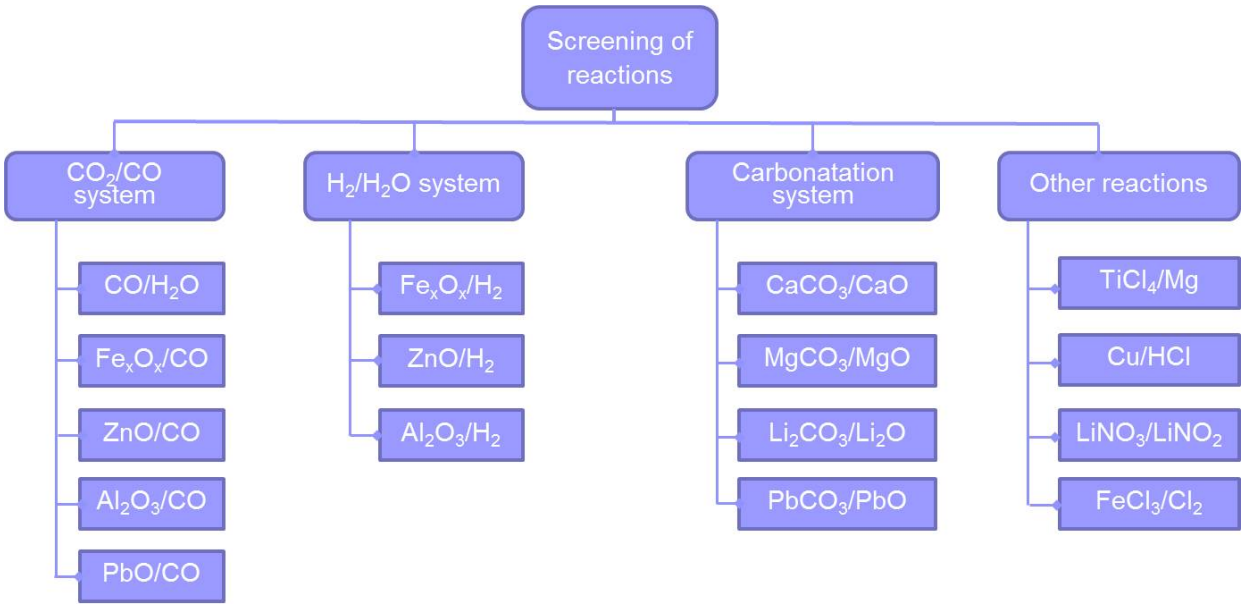

Figure 23. Screening analysis of thermochemical processes.

- Scale-up plants for thermochemical cycle

In addition to these STAGE-STE activities very relevant scale-up developments for TC-cycles have been performed in the framework of separate EU-projects and are briefly mentioned here:

(1) FCH JU project HYDROSOL PLANT involving STAGE-STE partners DLR and CIEMAT: A 750 kW_{th} plant upscaling the nickel-ferrites cycle for hydrogen production. The solar reactor has been designed, studied and built at DLR [16]. The erection of this plant on the SSPS tower of the Plataforma Solar de Almería (CIEMAT) has been completed and it is ready for start-up end of 2017. Two of the three reactors contain nickel-ferrite redox material; the third is equipped with Ceria foam.

(2) H2020 project SUN-to-LIQUID involving STAGE-STE partners ETHZ, IMDEA, DLR and ASNT: A 50 kW_{th} plant upscaling the dual porosity reticulate ceria ceramics cycle technology of ETHZ [17] for synthesis gas production. This plant has been installed in the new solar tower at IMDEA realised for this project. Characterisation and start-up activities for the heliostat field are ongoing end of 2017.

3.5 Alternative steam electrolysis for solar H_2 production

ENEA has built a lab-scale membrane reactor (volume 0.8 l) test-rig for medium temperature water electrolysis in molten alkali carbonates. Tests were carried out with the aim of selecting the membrane used to separate the anode and cathode space and prevent mixing of the produced gases. In this first phase, ceramic alumina porous membranes were considered. A Pt wire was used as anode, while the reactor wall served as cathode. The tests were carried out at ambient pressure, temperatures in the range 490-520 °C with a H_2O/CO_2 molar ratio in the feed equal to 1 (Fig. 24). The results indicate that the electrolysis can be carried out in the cell potential range 1.2-1.3. Steam conversions up to more than 20% were estimated. Significantly higher conversions can be expected once the reactor design is optimized.

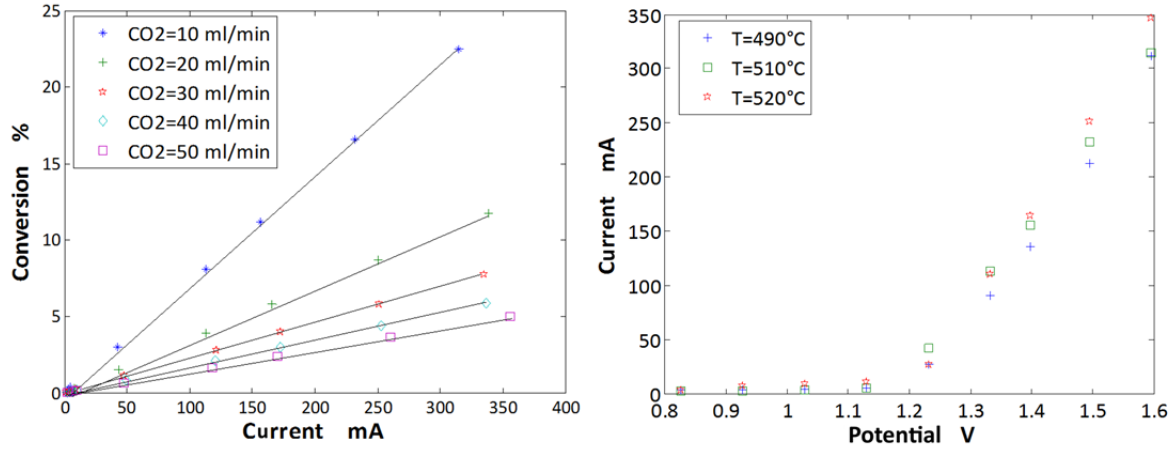

Figure 24. Laboratory tests for conversion and I-V characteristics of molten carbonate electrolysis cells.

Since a strong corrosion of the steel vessel was observed in these electrolysis tests a study of different alternative metallic materials was performed in ternary LiNaK molten carbonate at 500°C under CO_2 atmosphere using different electrochemical corrosion testing methods. The best performance was found for the FeAl intermetallic material Monel K400, followed by Inconel 600.

Based on these tests a new electrochemical cell reactor was designed and fabricated, as shown in Fig. 25. An alumina ceramic crucible (A) is inserted in a – as an intermediate solution - 316L steel vessel (B). The two compartments of the cell are separated by a porous separator (C). Steam is injected into the molten salt via a glass-ceramic sparger (D). 20 cm^2 sized planar electrodes from metallic meshes of copper and of Monel K400 are used. The cell power is about 1 W (1.2 V and 0.6-0.8 A). As a further step after the end of STAGE-STE it is planned to use Monel K400 also for the reactor vessel.

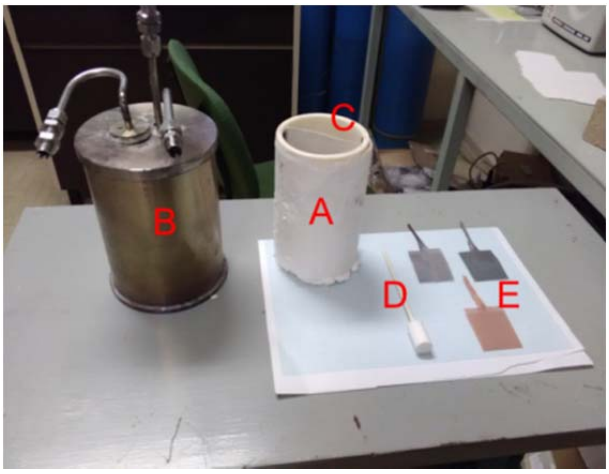

Figure 25. Components of the new electrochemical cell reactor realised at ENEA for testing molten carbonate electrolysis.

3.6 Thermochemical energy storage

CNRS has performed a literature survey on chemical materials that are potential candidates for thermochemical heat storage based on reversible redox reactions. The most promising and suitable thermochemical storage systems have been identified and selected as a function of temperature [18]. The evaluation of the selected systems was based on energy storage density, conversion rates, kinetics, reversibility, as well as general criteria such as toxicity and cost [19] and resulted in the selection of cobalt oxide and manganese oxide endothermal/exothermal redox systems for closer investigation. The potential improvement of their performance due to the addition of iron oxide is studied with thermogravimetric analyses methods. Fe addition is found to decrease the redox activity and energy storage capacity of Co_3O_4/CoO, whereas the reaction rate, reversibility and cycling stability of Mn_2O_3/Mn_3O_4 are significantly enhanced with added Fe amounts above ~15 mol%, and the energy storage capacity is slightly improved (Fig. 26) [20]. Furthermore the performance of Ba and/or Sr perovskites for thermochemical energy storage is investigated. As good candidates Sr-Fe and Sr-Co and even better Ba-Fe and Ba-Co perovskites were identified, while Sr-Mn and Ba-Mn perovskites are not suitable. Using both, Sr and Ba (namely Sr-Ba-Co and Sr-Ba-Fe perovskites), results in an additional positive effect. A case study on the integration of a manganese oxide based thermochemical energy storage system into a CSP plant leads to the conclusion that a thermochemical storage reactor should be designed in such a way that it can be integrated with the power block in a parallel configuration rather than a serial configuration.

Furthermore mixed metal oxides based on Cu-Mn-O, Cu-Co-O, and Mn-Co-O systems were synthesized via Pechini method, using commercial powders of the pure oxides as references. The influence of the addition of dopants to pure metal oxides on the cycling stability, the reaction temperature, and the heat storage capacity was investigated [21]. Cobalt oxide mixed with 10 mol%Cu was identified as a promising material showing a high reaction enthalpy and a relatively low gap in temperature between the reduction and the oxidation step of the cycle.

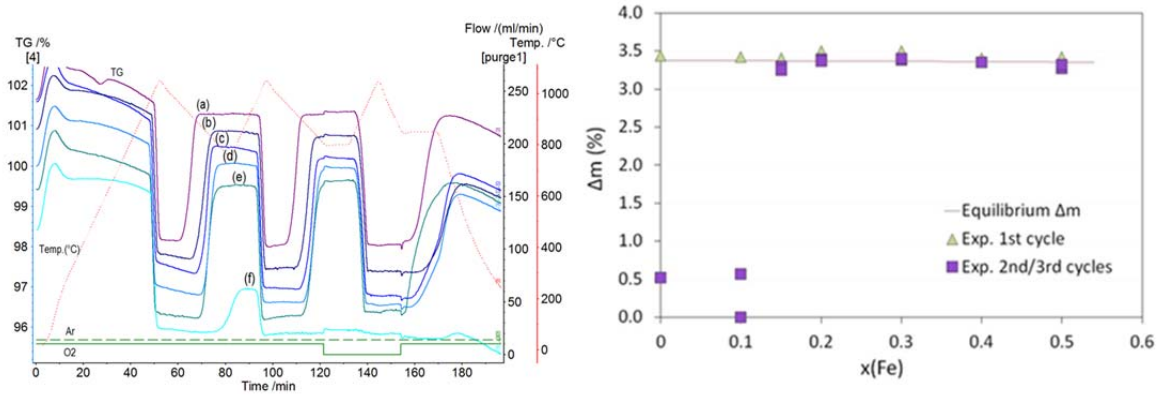

Figure 26. Left: TGA of Mn_2O_3/Mn_3O_4 with addition of (a) 50 mol% Fe, (b) 40 mol% Fe, (c) 30 mol% Fe, (d) 20 mol% Fe, (e) 15 mol% Fe, and (f) 10 mol% Fe; Right: Evolution of experimental Δm (%) during reduction compared to theoretical Δm (pO_2 = 0.20 atm).

A more detailed overview over most activities for thermochemical storage can be found in Deliverable 9.2.

3.7 References for Chapter 3

1. W. Villasmil, T. Cooper, E. Koepf, A. Meier, A. Steinfeld: Coupled ray-tracing, heat transfer, and thermochemical modeling of a 100-kW_{th} high-temperature solar reactor for thermal dissociation of ZnO, J. Solar Energy Eng. **139**(2), 021015-1/13, 2016. DOI:10.1115/1.4035330
2. W. Villasmil, A. Meier, A. Steinfeld: Dynamic modeling of a solar reactor for zinc oxide thermal dissociation and experimental validation using IR thermography, J. Solar Energy Eng. **136**, 011015-1/11, 2014. DOI:10.1115/1.4025511
3. M. Brkic, E. Koepf, A. Meier: Solar carbothermal reduction of aerosolized ZnO particles under vacuum: modelling, experimentation, and characterization of a drop-tube reactor, Chemical Engineering Journal **313**, 435–449, 2017. DOI:10.1016/j.cej.2016.12.057
4. N. Tzouganatos, C. Wieckert, A. Steinfeld: A packed-bed solar reactor for the carbothermal zinc production – dynamic modelling and experimental validation, AIChE Journal **62**, 4586-4594, 2016. DOI:10.1002/aic.15522
5. E. Koepf, W. Villasmil, A. Meier: High temperature flow visualization and aerodynamic window protection of a 100-kWth solar thermochemical receiver-reactor for ZnO dissociation, Energy Procedia **69**, 1780-1789, 2015. DOI:10.1016/j.egypro.2015.03.148
6. E. Koepf, W. Villasmil, A. Meier: Pilot-scale Solar Reactor Operation and Characterization for Fuel Production via the Zn/ZnO Thermochemical Cycle, Applied Energy **165**, 1004-1023, 2016. DOI:10.1016/j.egypro.2015.03.148

7. E. Koepf, W. Villasmil, A. Meier: Demonstration of a 100-kWth high-temperature solar thermochemical reactor pilot plant for ZnO dissociation, AIP Conf. Proc. **1734**, 120005, 2016. DOI:10.1063/1.4949207

8. C.A. Cerpa, J. Gonzalez-Aguilar, M. Romero: Diseño y construcción de un banco de ensayos de tipo "beam-down" para estudios de termoquímica solar: reducción de ceria, Proceedings XI Congreso Iberoamericano, Queretaro, Mexico, 6-10 October 2014. Ed. A. Lentz. Pub. ANES, Mexico, 1501-1508.

9. L. Arribas et al.: Development of a solarized rotary kiln for High-Temperature chemical processes, Solar World Congress 2015, Daegu, Korea, November 8-12, 2015.

10. M. Brkic, E. Koepf, A. Meier: Continuous Solar Carbothermal Reduction of Aerosolized ZnO Particles under Vacuum in a Directly Irradiated Vertical-Tube Reactor, J. Solar Energy Eng. **138**(2), 021010-1/14, 2016. DOI:10.1115/1.4032685

11. A. T-Raissi, N. Muradov, C. Huang, O. Adebiyi: Hydrogen from solar via light-assisted high-temperature water splitting cycles, J. Solar Energy Eng. **129**(2), 184-189, 2007. DOI:10.1115/1.2710493

12. A.C. Tizzoni, N. Corsaro, C. D'Ottavi, S. Licoccia, S. Sau, P. Tarquini: Oxygen production by intermediate metal sulphates in sulphur based thermochemical water splitting cycles, Int. Journal of Hydrogen Energy **40**(11), 4065-4083, 2015.

13. F. Varsano, M.A. Murmura, B. Brunetti, F. Padella, A. La Barbera, C. Alvani, M.C. Annesini: Hydrogen production by water splitting on manganese ferrite-sodium carbonate mixture: Feasibility tests in a packed bed solar reactor-receiver, Int. J. Hydrogen Energy **39**, 20920-20929, 2014.

14. M.A. Murmura, F. Varsano, F. Padella, A. La Barbera, C. Alvani, M.C. Annesini: Hydrogen production by the sodium manganese ferrite thermochemical cycle - experimental rate and modeling, Ind. Eng. Chem. Res. **53**(25), 10310–10317, 2014. DOI:10.1021/ie500940z

15. M. Ezbiri, K. Allen, M. Gàlvez, R. Michalsky, A. Steinfeld: Design Principles of Perovskites for Thermochemical Oxygen Separation, ChemSusChem **8**, 1966-1971, 2015. DOI:10.1002/cssc.201500239

16. J.-P. Säck, S. Breuer, P. Cotelli, A. Houaijia, M. Lange, M. Wullenkord, C. Spenke, M. Roeb, C. Sattler: High temperature hydrogen production: Design of a 750 KW demonstration plant for a two step thermochemical cycle, Solar Energy **135**, 232-241, 2016. DOI:10.1016/j.solener.2016.05.059

17. D. Marxer, P. Furler, M. Takacs, A. Steinfeld: Solar thermochemical splitting of CO_2 into separate streams of CO and O_2 with high selectivity, stability, conversion, and efficiency, Energy & Environmental Science **10**(5), 1142-1149, Cambridge: Royal Society of Chemistry, 2017. DOI:10.1039/C6EE03776C

18. L. André, S. Abanades, G. Flamant: Screening of thermochemical systems based on solid-gas reversible reactions for high temperature solar thermal energy storage. Renewable & Sustainable Energy Reviews **64**, 703-715, 2016. DOI:10.1016/j.rser.2016.06.043

19. A. H. Abedin and M. A. Rosen: A critical review on thermochemical energy storage systems, The Open Renewable Energy Journal **4**, 42-46, 2011.

20. L. André, S. Abanades, L. Cassayre: High-temperature thermochemical energy storage based on redox reactions using Co-Fe and Mn-Fe mixed metal oxides, J. Solid State Chem 253, 6-14, 2017. DOI:10.1016/j.jssc.2017.05.015.

21. L. André, S. Abanades, L. Cassayre: Mixed Co, Cu and Mn-based metal-oxides for thermochemical energy storage applications, SolarPACES 2017 Conference, Santiago de Chile, September 26-29, 2017.

4. Task 9.3 “Innovative materials for next generation solar chemical reactors“

Thermochemical processes require thermally and chemically stable reactor wall materials that can withstand severe operating conditions of specific solar fuel production processes.

This task has been led by CNRS with the further participants CIEMAT, PSI, LNEG and IMDEA. Key information of insights and results gained in this Task can be found in the two milestone reports MS 36 and MS38 and in the Deliverable report D9.3.

4.1 Materials development

PSI focused its work on the realization of a windowless version of the indirectly heated two-cavity packed bed solar reactor. A modified version of PSI’s 5 kW lab scale reactor has been realized allowing for gas-tight mounting of the emitter plate (see Figure 27). Crucial issues are the sealing at sealing temperatures of around 1000°C and the identification of emitter materials and shapes that are chemically and mechanically (no cracking) stable at the severe operating conditions. Successful windowless tests were performed with carbon fiber reinforced SiC and with SSiC, first for carbothermal reduction of ZnO to Zn. Then, the solution was demonstrated with steam gasification of carbonaceous feedstock [1].

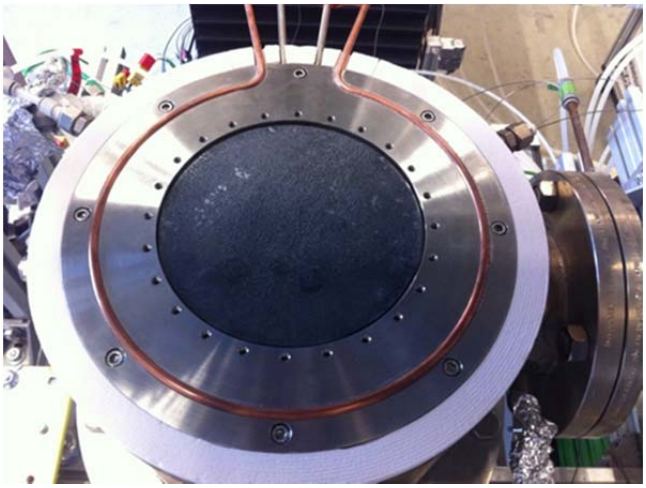

Figure 27. Emitter plate from C-fiber reinforced SiC (diameter 15 cm) mounted in the new gas tight sealing structure, as used for the first successful windowless tests with the indirectly heated packed bed solar lab reactor

LNEG developed an innovative material: semi-closed open cell ceria foams for ceria-based thermochemical cycles with a high specific surface area and gas tortuosity [2-3]. It was distributed to partners involved in WP9. These foams were made by the replication method using polyurethane foams as templates. Sintering was carried out in air at 1500ºC for 30 min. Brown alumina foams were also produced using the same technique and have been evaluated at CIEMAT-PSA (Figure 28).

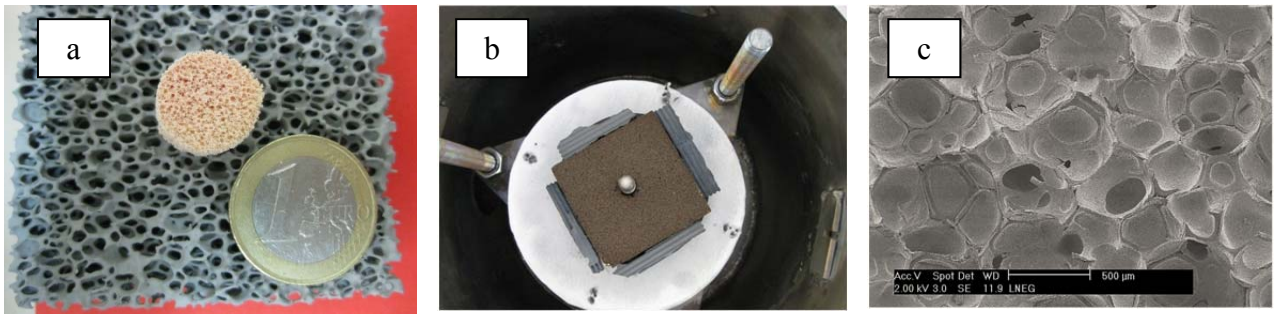

Figure 28. Semi-closed open cell ceria (a) and brown alumina (b) foams and their structure (c)

IMDEA Energy focused its activity on synthesis, shaping and characterization of active materials for solar reactors, mainly particles/pellets and foams, which could be applied for solar fuels production and thermochemical heat storage. Metal oxide mixtures obtained by mechanical milling of Mn_3O_4 and CeO_2 powders as a function of mechanical milling procedure, Mn_3O_4/CeO_2 ratio and synthesis atmosphere have been analyzed. X-Ray diffraction showed that oxide mixtures preserved segregated phases, so that no chemical reaction between the metal oxides seemed to be produced. Cyclability under thermal cycles has been studied in the temperature range between 550 and 1000 °C, as shown in Figure 29. In this interval, chemical reactivity is only related to manganese oxide contribution.

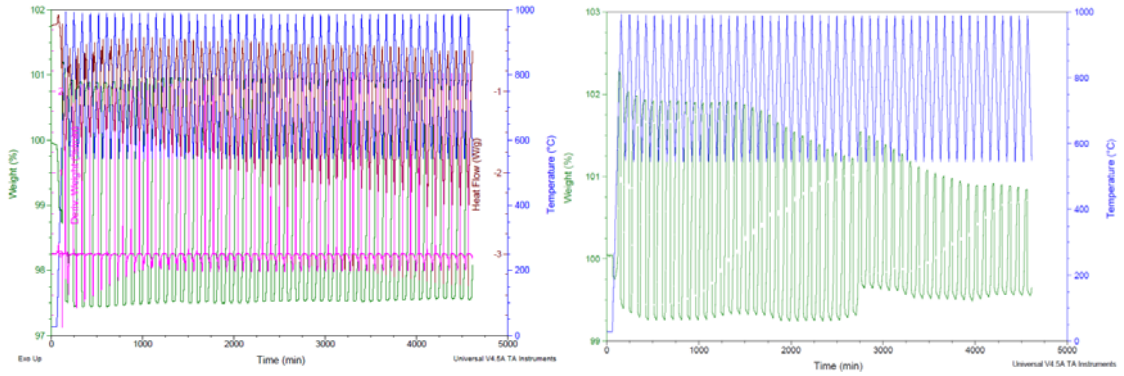

Figure 29. Cyclability test using pure Mn_3O_4 (left) and a metal oxide mixture 75Mn/25Ce (right).

4.2 Materials characterisation

CNRS has developed the DISCO setup (Figure 30) in order to measure the reflectance/absorbance in the solar spectrum of materials. This facility was also used in WP8 and is available for on-sun characterization of metal and ceramic materials.

Figure 30. The DISCO setup. An optical fibre emits a solar beam perpendicular to the surface of the sample placed at the focus of a solar furnace, while eight fibres collect the reflected flux in different directions, from 0° to 70°.

CNRS performed measurements of optical properties variation of Tantalum carbide (TaC) after high temperature oxidation. TaC could be an interesting candidate for manufacturing a selective emitter plate e.g. for in the two-cavity reactor developed by PSI due to its very good spectral selectivity, which could be increased by surface treatments and microstructuring. However, Ta_2O_5 presents the opposite selectivity. Therefore, CNRS investigated the oxidation of TaC in air and in helium at 1100 K and determined the impact of this oxidation on the optical and thermal properties using reflectivity and bidirectional reflectance distribution function (BRDF) measurements and laser flash analysis (LFA), respectively. It was observed that the oxidation in air was too severe. Additionally, the samples treated in helium were sufficiently oxidized by the residual oxygen to lose their spectral selectivity.

The experiments performed using the REHPTS reactor (developed for accelerated ageing tests) have demonstrated that TaC is very sensitive toward oxidation. A 20 min plateau at 1100 K in air is sufficient to produce an oxide layer that peels off during cooling. XRD and Raman characterization show that the fragmented oxide layer is made of orthorhombic Ta_2O_5, whereas very little oxide is present on the remaining disk. During a 20 min plateau at 1100 K in helium, an oxide layer was also formed as proved by the slight weight variation and the post-experimental SEM coupled with EDS and profilometry analysis, both showing the initial surface of the sample (with scratches and grains) covered by a 25 µm-thick oxide layer. This modification is sufficient to affect the thermal and optical properties of the sample.

Room temperature optical properties were measured using a Perkin Elmer Lambda 950 and an SOC 100 hemispherical directional reflectometer (SOC 100 HDR). The Perkin Elmer Lambda 950 measures normal hemispheric reflectivities on a range of wavelengths from 250 to 2500 nm. The SOC 100 HDR enables the determination of the hemispherical directional reflectance on the interval from 2 to 25 µm. Figure 31 plots the variation of the sample reflectance before and after oxidation tests. Consequently, at 1100K the absorber thermal efficiency decreases from 55% (initial TaC) to about 25% (oxidized TaC). The resulting loss of solar reactor thermal efficiency is illustrated in Figure 32.

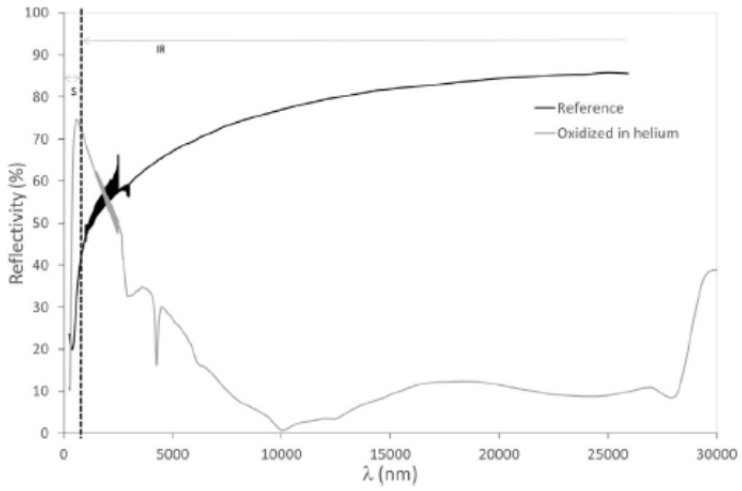

Figure 31. Room temperature normal reflectance according to the wavelength for reference TaC and for oxidized TaC at 1100 K for 20 min in helium. The dotted line is separating the areas corresponding to the solar spectrum (S) and to the infrared re-emission (IR).

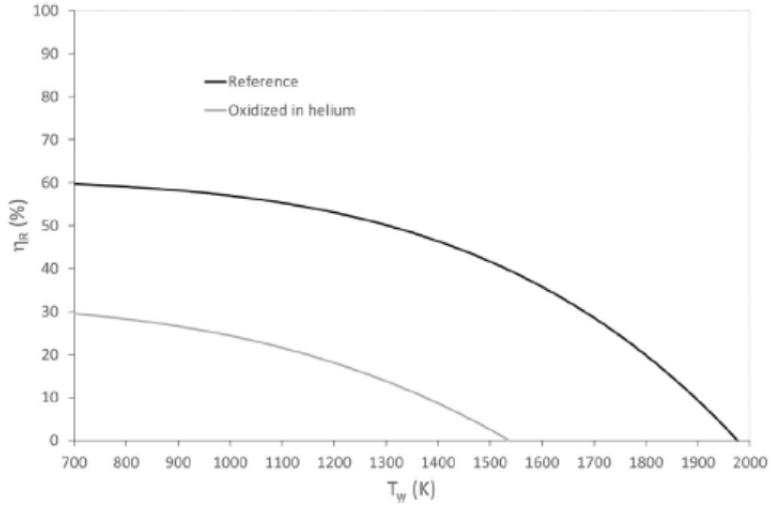

Figure 32. Reduction of reactor efficiency due to the change of optical properties after oxidation as a function of temperature.

4.3 Accelerated aging and durability tests

CNRS, CIEMAT, PSI, LNEG, and IMDEA have developed a durability test methodology to qualify innovative materials for next generation solar chemical reactors.

The proposed durability test methodology is based on the expertise available in ageing tests of conventional porous gas burners (LNEG) as well as in ageing tests of components and materials for solar reactors using concentrated solar radiation (CNRS and CIEMAT).

Figure 33 shows a flowchart of the proposed durability test methodology. The main purpose is to (1) identify most suitable accelerated test conditions to qualify materials for solar

chemical reactors, (2) select specific material properties to assess damage over time and cycles, and (3) develop a durability test protocol.

The proposed durability test methodology includes:

- Selection of test materials
- Reactor design
- Ageing test procedure
- Damage assessment
- Reactor and materials modelling
- Validation of materials, models, and methodology
- Lifetime prediction

This report presents concise information concerning the following items:

- Materials selection criteria
- Reactor design criteria
- Equipment for lifetime prediction methodology
- Procedures for performing ageing tests
- Procedures for processing and interpretation of ageing test results

Specific equipment for performing durability tests have been identified and used during the project execution. Figures 34 and 35 give examples of these devices:

Figure 34 illustrates the REHPTS (Réacteur Hautes Pression et Température Solaire – High Pressure and Temperature Solar Reactor) reactor installed at the focus of the 6 kW vertical axis solar furnace at the PROMES-CNRS laboratory in Odeillo.

The Solar furnace team at PSA has designed and manufactured a new vacuum chamber called “Dome chamber” (Figure 35), which is adapted to the power and size of the focus of the PSA SF-60 solar furnace [4-5].

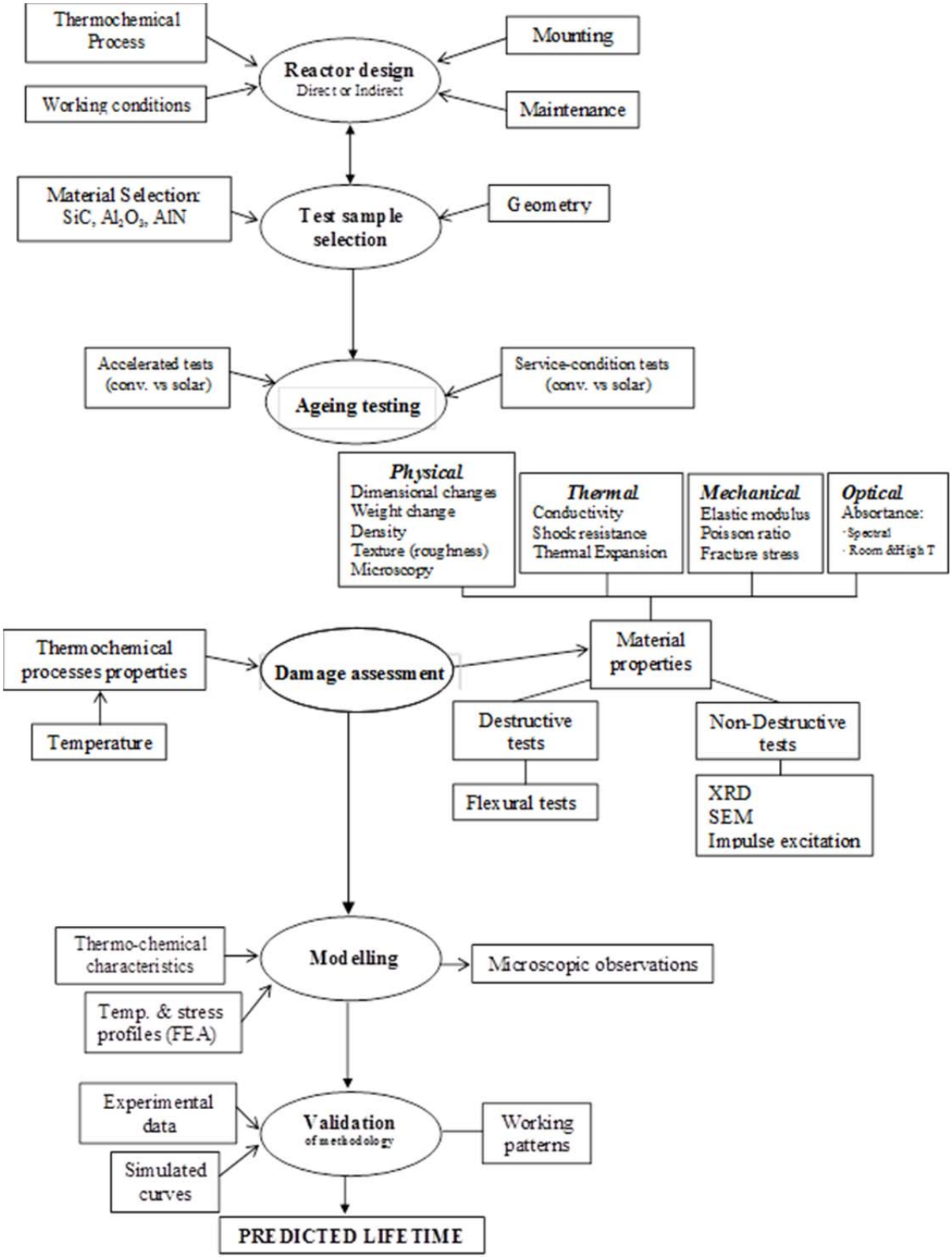

Figure 33. Flowchart of proposed durability test methodology.

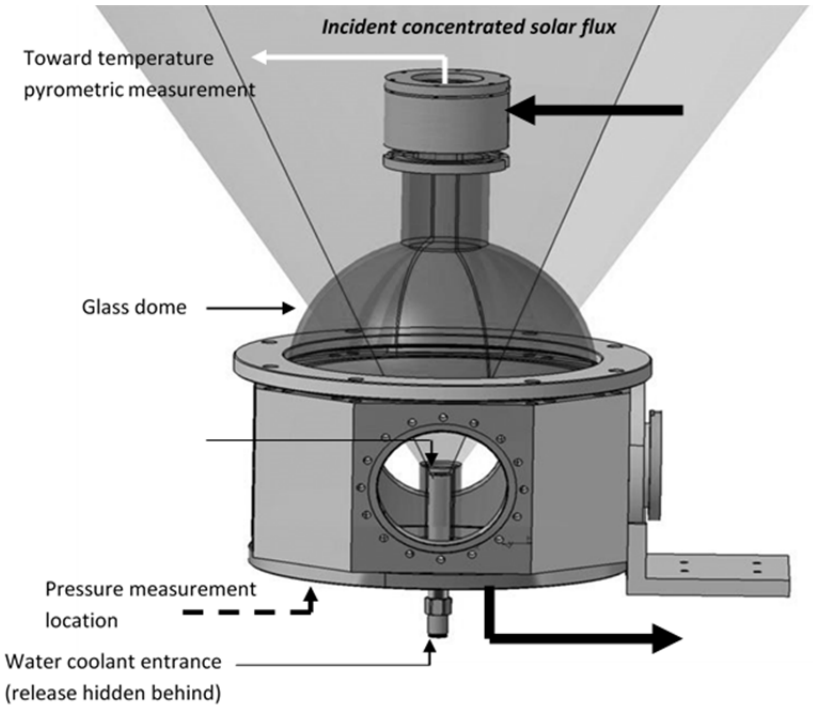

Figure 34. Schematic of the CNRS REHPTS reactor.

Figure 35. The PSA SF-60 solar furnace (left) and the Dome chamber (right)

Example of typical experimental results

Iron oxide-coated mullite, brown alumina and ceria foams prepared at LNEG (see Chapter 4.1) were subjected to cycling heating under well-controlled conditions at CIEMAT-PSA up to 100 cycles (Figure 36). Temperature differences ranging from 200 K (700-900 °C); 400 K (700-1100 °C) and 600 K (700-1300 °C) were selected. Concerning active RCP, ceria, which undergoes high catalytic activity towards H_2 production, showed good thermal shock resistance behavior after thermal cycling in the temperature range 700-1300 °C, which makes it an attractive material for thermochemical fuel production. Damage assessment was evaluated by means of scanning electron microscopy and compressive mechanical testing.

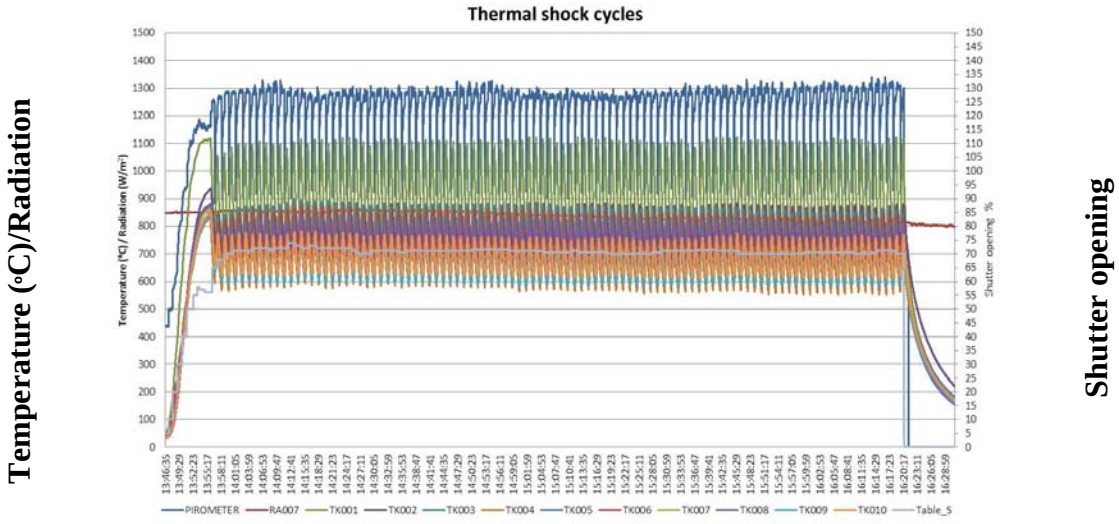

Figure 36. Temperature profiles obtained for thermal shock tests at ΔT=400 K

These results suggest that these RPC ceria is an attractive material for thermochemical fuel production that undergoes high catalytic activity towards H_2 production, with an excellent thermal stability, and an ability to maintain structure under aggressive thermal cycling.

Ageing studies of wall materials has been performed at PROMES-CNRS. AlN and SiC/SiC_f have supported cyclic oxidations with temperature dwells from 1370 to 2100 K. The investigations lead to the experimental determination of semi-parabolic kinetic constant k_p, correlated to the temperature through an Arrhenius law: $k_p = Aexp\left(-\frac{E_a}{RT}\right)$. For AlN and SiC/$SiC_f$, the experimental values for the activation energy are respectively 221 and 336 kJ mol^{-1}.

Table 5 provides an overview over most of the material investigations performed with Task 9.3 of STAGE-STE. More details are to be found in the MS38 report (see reference in first column).

Reference	Material tested	Variables measured	Main Instrumentation	Boundary Conditions
Milestone M38 STAGE-STE Project Section 2.1.1	AlN ageing tests in air	Weight Loss Micro-Raman Spectroscopy XRD analysis Kinetic analysis.	Solar Facility at PROMES laboratory (Odeillo)	Isothermal heating 60 min. at 1600 K; Cycles from 1600 to 2000 K Exposure time: 20 min and 5 min (cooling period).
This report Chapter 4.2	TaC	Optical reflectance (oxidized and non-oxidized)	REHPTS-reactor Reflectometer XRD, SEM/EDS; Raman	Before and after 20 min at 1100 K in air and He
Milestone M38 STAGE-STE Project Section 2.1.4	Al_2O_3	Thermodynamic simulation (GEMINI software)		
Milestone M38 STAGE-STE Project Section 2.1.5.	Iron-coated mullite foams	Visual inspection	Solar Accelerated Aging Facility at PSA	Cyclic irradiance at 600, 800 and 1000 ºC
Milestone M38 STAGE-STE Project Section 2.1.2.	SiC/SiC_f	Visual Inspection XRD analysis SEM Weight loss Micro-Raman Spectroscopy	Solar Accelerated Aging Facility at PROMES laboratory (Odeillo)	Cycles from 1600 to 2000 K Exposure time: 20 min and 5 min (cooling period).
Milestone M38 STAGE-STE project Section 2.1.5	SiC plates	Visual Inspection	Solar accelerated aging facility at PSA	Cyclic irradiance of average at 1050ºC
Milestone M38 STAGE-STE Project Section 2.1.3	SiC/SiC_f	O_2 and H_2 releasing	Solar Accelerated Aging Facility at CIEMAT laboratory	Cycles at 1200ºC. Exposure time: 2h
Milestone M38 STAGE-STE Project Section 2.2.2	CeO_2 RPC monolith	O_2 and H_2 releasing	Solar Accelerated Aging Facility at CIEMAT laboratory	3 cycles at 1400ºC (reduction) and 1200ºC hydrolysis
Milestone M38 STAGE-STE Project Section 2.2.1	CeO_2 RPC accelerated ageing tests	Visual Inspection	Solar Accelerated Aging Facility at PSA	Up to 150 thermal cycles at 700ºC and 1100ºC
Milestone M38 STAGE-STE Project Section 3.1	CVD-SiC coating on graphite (windowed) SSiC, SiC/C_f (windowless)	Weight loss Visual inspection	Solar Facility at PSI laboratory (Switzerland) Two cavity solar lab reactor	Cycling studies at operating conditions

Table 5. Overview over materials investigations in Task 9.3.

4.4 References for Chapter 4

1. C. Wieckert, N. Tzouganatos, A.Steinfeld: Demonstration of a 5kWth windowless packed-bed reactor for high temperature solar thermochemical processing, in SolarPaces Conference 2017, Santiago de Chile, (anticipated) publication in AIP conference series, 2018.
2. R.C. Pullar, L. Gil, F.A.C. Oliveira: Biomimetic cork-based CeO_2 ecoceramics for hydrogen generation using concentrated solar energy. Ciência & Tecnologia dos Materiais **28**(1), 23-28, 2016. DOI:10.1016/j.ctmat.2016.04.002
3. R.C. Pullar, R.M. Novais: Cork-based biomimetic ceramic 3-DOM foams. Mat. Today **20**(1), 45-46, 2017. DOI:10.1016/j.mattod.2016.12.004
4. B. Li, F.A.C. Oliveira, J. Rodríguez, J.C. Fernandes, L.G. Rosa: Numerical and experimental study on improving temperature uniformity of solar furnaces for materials processing, Solar Energy **115**, 95–108, 2015. DOI:10.1016/j.solener.2015.02.023
5. F.A.C. Oliveira, J.C. Fernandes, J. Rodríguez, I. Cañadas, J. Galindo, L.G. Rosa: Temperature uniformity improvement in a solar furnace by indirect heating, Sol. Energy **140**, 141–150, 2016. DOI:10.1016/j.solener.2016.11.004

5. Task 9.4 “Technology assessment of solar thermochemical fuel production“

The objective of this task led by DLR with further partners CIEMAT, PSI, ENEA, UEVORA and IMDEA was to evaluate different routes for thermochemical production of solar fuels, to investigate technological options for the integration of various solar fuels production processes and to prepare a technology roadmap to describe essential RTD requirements to further develop solar thermochemical fuels processes.

5.1 Technology integration

This task is mainly dedicated to the technology integration and technology assessment of solar fuel production. The analysis consists of the elaboration of flowsheets, the integration of CSP technologies and the simulation and the techno-economic analysis of the overall process. Thermochemical cycles to split water into hydrogen and oxygen have the potential to basically avoid any CO_2 emissions. The first idea mentioned in the DoW of the STAGE-STE project was to consider in Task 9.4 only solar thermochemical water splitting cycles for hydrogen production and a screening has been performed to identify the most suitable thermochemical cycles for hydrogen production. However, based on their development level and local or regional prioritization also solar driven steam electrolysis and solar processes based on carbonaceous feedstocks were investigated. It has been thus decided by the project partners involved in T9.4 to take into consideration the following processes within the analysis:

- Solar thermochemical cycles (non-volatile metal oxide cycle, ZnO/Zn cycle and hybrid sulphur cycle)
- Solar driven solid oxide steam electrolysis
- Molten carbonate steam electrolysis
- Solar steam reforming at high temperature and at low temperature molten salt heated
- Solar gasification of carbonaceous materials and wastes
- Solar molten salt heated hydrothermal liquefaction of wet biomass

Solar energy concentrating technologies able to deliver heat and electricity were identified and investigated in the report for MS 37 in order to assess their compatibility with the processes defined.

Concept schemes and flowsheets have been developed and simulations have been carried out with Aspen Plus® and Ebsilon Professional softwares for the different process investigated for hydrogen production rate of 400 kg and 4000 kg per day. Economic studies have been

carried out considering a lifetime of the plant of 25 years and an annual effective interest rate of 8%.

The concepts, flow sheets and economic analysis results of the technology assessment of the processes listed above have been described in detail in the Deliverable D9.4 “Final report on “Technology Roadmap for Solar Fuels””.

For the non-volatile metal oxide cycles, the cycles based on ferrites and most recently ceria have received most attention [1].

For the ZnO/Zn cycle the technology assessment considerations are mostly based on the rotary cavity design for the solar ZnO dissociation reactor followed by a gas quench. Respective technology assessment work has been conducted by [2-8], with [8] basing on [2] and [5]. The most recent work is by Koepf and Jakober [9].

The technology assessment activities of the carbothermal ZnO/Zn cycle are based on [10, 11]. A more detailed overview of this development is to be found in [12]. Anticipated costs of upscaled plants based on this solar reactor concept have been estimated [10, 11].

Concept scheme and flow sheets [13] have been developed for a solar driven hybrid sulphur cycle process. For the supply of medium temperature heat, a parabolic trough CSP plant using solar salt as heat transfer and storage medium was considered; 8 h of daily operation were assumed with 16 h of heat storage in order to allow for continuous operation (in nominal conditions) for the process units that rely on this type of energy input. A central receiver CSP plant was considered to provide high temperature heat, which is only needed for sulphuric acid decomposition; 8 h of daily operation and no heat storage were considered in this case, so that sulphuric acid decomposition and, consequently, sulphuric acid vaporization and unreacted SO_3 separation are assumed to operate discontinuously, only at daytime. An economic study has been carried out considering multiple scenarios [14].

Flowsheeting and simulations of solar steam reforming [15, 16] have been carried out as well as an economic study.

The system analysis for low-temperature MS (molten salt)-heated reforming is based on a membrane reactor and considers CH_4 as reformable feedstock. In the process analysis, the plant is assumed to operate continuously using heat from the hot MS stream coming from the solar plant: when solar energy is not available and the heat storage of the concentrated solar thermal plant is depleted a backup fuel fired heater to heat the MS [17]. Different reactor architectures were assumed for the different plant capacity. Further information can be found in the final summary report of the CoMETHy project [18].

The coupling of the solid oxide steam electrolysis with molten salt solar tower technology as solar energy source has been studied in detail including a thermal storage [19]. In alternative scenarios, the CSP system is only required for heat supply. Thus, based on its simplicity and the low cost of the components, a Linear Fresnel Reflector with thermal oil as heat transfer fluid was selected. The simulation of the processes was carried out with the commercial

simulation tool Ebsilon Professional to calculate energy and mass balances for a production of 400-600 kg/day hydrogen, which is sufficient to fuel about 20 buses [20].

An optimized integration scheme of molten carbonate steam electrolysis with a solar energy source has been identified and a process analysis of molten carbonate electrolysis was carried out for different scenarios. The analysis showed that due to a good potential for heat recovery medium temperature heat has just a very small share of the total energy required by the process. Medium temperature heat is not even required if the electrolysis is carried out slightly above the thermo-neutral potential (~1.28 V at 500°C). Thus despite high temperature operational requirements of molten carbonates electrolyser (500 ºC – 600 ºC), electrolysis exothermic behavior reduces the external heat addition needed by solar energy source. Thermochemical efficiencies approaching 30 % were estimated for the process in case high steam conversion (above 70%) can be achieved with a further optimization of the process configuration.

The solar gasification of carbonaceous materials and wastes process has primarily been developed for production of syngas for direct combustion (e.g. in a cement kiln) or eventually for further processing to liquid fuels and has been studied intensively in several solar reactor types [21]. Since here the focus is on the production of solar hydrogen, a shift reactor and a PSA have been added.

A conceptual analysis of the coupling of a concentrating solar power plant, based on parabolic through technology, with a plant for hydrothermal liquefaction of wet biomass was done under the constraint of maximizing the thermal recovery from the hot reactor effluent. Part of the process heat is supplied by a molten salt stream, used as heat transfer fluid and heated by the solar plant that is equipped with a storage tank of hot molten salt as thermal energy storage system. The process layout is based on the apparatus used in experimental studies on the hydrothermal conversion of microalgae and ligno-cellulosic biomass in continuous lab-scale reaction systems [22-25].

5.2 Technology roadmap of solar fuels

Following the assessment of the different solar fuels production processes, a technology roadmap was prepared with recommendation for future R&D priority work including a list of development areas to foster further development of solar fuels production processes and to facilitate scaling up the solar fuels technologies in a fast and efficient way. This roadmap is presented in the Deliverable D9.4 “Final report on “Technology Roadmap for Solar Fuels””. Research priorities are proposed in order to improve the solar fuels production processes to get closer to their theoretical efficiency limits. Larger scale demonstration activities are necessary to get the technologies closer to market application, as well. The following step is the first market introduction which will prepare the entry into the market learning curve that will finally lead to the cost reduction to be competitive. This roadmap includes new processes (i.e. molten carbonate electrolysis) which have not been investigated within previous

roadmaps and which were selected here because of their interesting and promising first results.

Non-volatile metal oxide cycles presently are in the TRL range of 5-6. The achieved developments are very promising for a fast deployment of this technology. The current challenges concerning the thermal management and the gas separation appear to be solvable in the mid-term future. Present solar towers for power production are designed for much lower temperatures and therefore concentrations. Solar towers for fuel production must achieve concentration factors of over 2000 and need a control strategy that prevents temperature variations in the receiver-reactor to operate the chemical process efficiently. The receiver reactors must be further developed to minimize inert heated mass like structures and flushing gases. Also more active redox materials need to be developed. To solve the challenges on the conventional part, detailed transient models should be employed to predict the performance of alternative concepts of thermal management.

Concerning the carbon-free ZnO/Zn thermochemical cycle process major issues have been identified in the research up to now. These specifically include in the currently explored approach for separation of Zn and O_2 requiring a large amount of inert gas for quenching the Zn(g)-O_2-mixture and - related to this - the need to separate the inert gas from O_2. Guided by this it is suggested not to focus on this research line in larger scale as long as no breakthrough technology option regarding Zn-O_2 separation and/or inert gas-O_2 separation has been identified. However it appears to be justified to foresee a limited activity to search for such breakthrough technology options.

The carbothermal ZnO/Zn cycle avoids these issues due to the production of a gas mixture of Zn(g) and CO well known in Zn metallurgy. However although the pilot scale carbothermal ZnO reduction tests (TRL 5-6) were quite successful, no direct follow up activity could yet be realized. Now, that major issues with the ZnO dissociation cycle have been identified, the reconsideration of the carbothermal ZnO cycle appears to be advisable. Three types of R&D work are recommended: work for improvement of the solar reactor, further development of the hydrolysis step and a basic study of a more direct path to solar H_2 via this cycle. Regarding further test installations and scale-ups, it is recommended to start a new initiative to win industrial partners for scaling-up of this technology by reactivating old industry contacts and by initiating new ones. The realization of a prototype demonstration at the level of a few MW should be targeted.

The solar heated hybrid sulphur cycle has actually achieved a TRL of 5 and is a very promising technology for solar hydrogen production. This TRL could increase by larger scale demonstration activities with further scaling of the sulphuric acid splitting section in the MW-range. Other factors to be further researched is the pressurization of the sulphuric acid splitting reactor (e.g. 10 bar), the development of a suitable high temperature heat storage (i.e. 900 °C) for continuous operation of the sulphuric acid splitting as well as the development of the heat recovery system between outlet (850 °C) and inlet of sulphuric acid splitting as well as the gas separation after sulphuric acid splitting for efficient recovery of O_2 as by-product/off-gas. Regarding the sulphur dioxide electrolyser (SDE) section, it has to be further

optimized to avoid/reduce/control the sulphur formation. This SDE should be further scaled-up and on-field demonstrated at relevant scale. Another development factor is the pressurization of SDE (e.g. 10-20 bar). Concerning the materials development, research on optimization of the catalysts for sulphuric acid splitting has to be done as well as research on protective coating to reduce corrosion of steel components in sulphuric acid splitting reactor.

The solar steam reforming has actually a TRL of 5-6, which is very promising for a further deployment of this technology. Industrial partners from different areas have to be involved in Sunbelt countries to build a demonstration plant to achieve TRL 7. Demonstrated on such a level the plant can be optimized and the system can be tested and qualified in operational environment.

The solid oxide electrolysis (SOE) coupling with solar concentrated energy is a highly promising technology for future hydrogen production. SOE systems need to be developed closer to commercial hydrogen production. This means larger cells and stacks as well as long term operation tests and coupling to appropriate heat sources. With an increasing hydrogen demand for mobility and industry the SOE coupled with CSP could play a big role in renewable hydrogen production. Until now the FCH JU has provided noticeable R&D support to this technology, leading to more efficient and durable units. Durability beyond 10,000 h and efficiencies above 80 % are the main priorities in the roadmap of the technology by 2030, together with scaling up of stacks and integration of replicating units with different energy sources, among them concentrating solar thermal. Follow up projects should target the demonstration of SOE units with solar thermal plants.

The technological maturity of the molten carbonate steam electrolysis is currently low (TRL 3) and the available information on the process was obtained in preliminary experimental campaigns with commercial molten carbonate fuel cell operated in electrolysis conditions and with an alumina crucible laboratory cell. Therefore, the short to medium-term R&D efforts should be focused on raising the TRL to at least 5 by developing and testing a significant scale electrolyser prototype in relevant operating conditions. To that end, one of first issues to be solved is the selection of appropriate corrosion resistant materials both for the electrolyser shell and for the electrodes; such materials must be able to withstand corrosion in the harsh molten carbonate environment for long operating times. Indeed, the preliminary tests on reversed molten carbonate fuel cell suggested that the conventional electrode materials used for such devices may not be suitable for operation in electrolysis mode. Once the materials will be selected, it will be possible to realize and test new laboratory reactors which will allow studying the process under more realistic conditions. Further work is required also on the system analysis and integration side. Gas handling and separation operations required downstream of the electrolyser are energy consuming and currently bottleneck the efficiency of the process. New solutions should therefore be evaluated for this section. In parallel, alternative uses of the electrolyser outlet gases, which avoid CO_2 separation, should be evaluated. Furthermore, the integration strategy of molten carbonate steam electrolysis with CSP plants should be optimized.

Concerning the solar gasification of carbonaceous materials and wastes, the promising results of the tests so far on TRL 5-6 level as well as the simplicity and versatility of the reactor design offering the potential to convert basically all carbonaceous materials to high quality syngas without major pretreatment qualifies this process for a further development. Two topics of specific interest to be studied are the following: first the realization of a transport of the feedstock into a hot reactor, thereby making a tar cracker, which is currently required for certain feedstock during the heat-up phase of the reactor, obsolete. An interesting realization of this might make use of a pushing furnace principle. Another major improvement compared to the demonstrated state of the art concerns the omission of the quartz window. Instead of the established sealing of the reactor towards ambient air at the water-cooled holding structure of the window, in this case the sealing has to be performed at the ceramic absorber. Furthermore, the absorber material must be stable in air as well as the gasification gas at up to about 1400°C and withstand the mechanical stresses due to thermal gradients etc. Such a windowless design has been successfully demonstrated on lab-scale using differently shaped absorbers from different materials [26]. The successive logical step would then be the design and realization on pilot scale. This provides further challenges like the ones caused by the limited ceramic sizes available for the solar absorber.

Even if the solar molten salt heated hydrothermal liquefaction of wet biomass process to not lead to hydrogen production it offers several advantages, with respect to traditional non-solar processes or to the most studied solar reactors to use solar heat to perform chemical processes. Indeed wet biomass containing streams (also waste biomass) can be converted into renewable biofuels; continuous operation is possible to produce large amount of fuel commodity and high pressure (up to 30 MPa) processes can be performed, due to the physical separation between the plant section devoted to the reaction (reactor) and that used for solar heat storage and transfer (molten salt stream). For the development of this technology from TRL 2-3 to higher TRL values, it is considered necessary to investigate the process in lab-scale continuous systems heated by molten salts, to investigate the design of the solar plant to adapt it to the chemical process and to prepare demonstrative plants at small scale to demonstrate technological feasibility in operational environment.

The proposed R&D actions for these processes are summarized in the roadmap presented in Fig. 37. Fig. 38 shows the scale-up strategy roadmap.

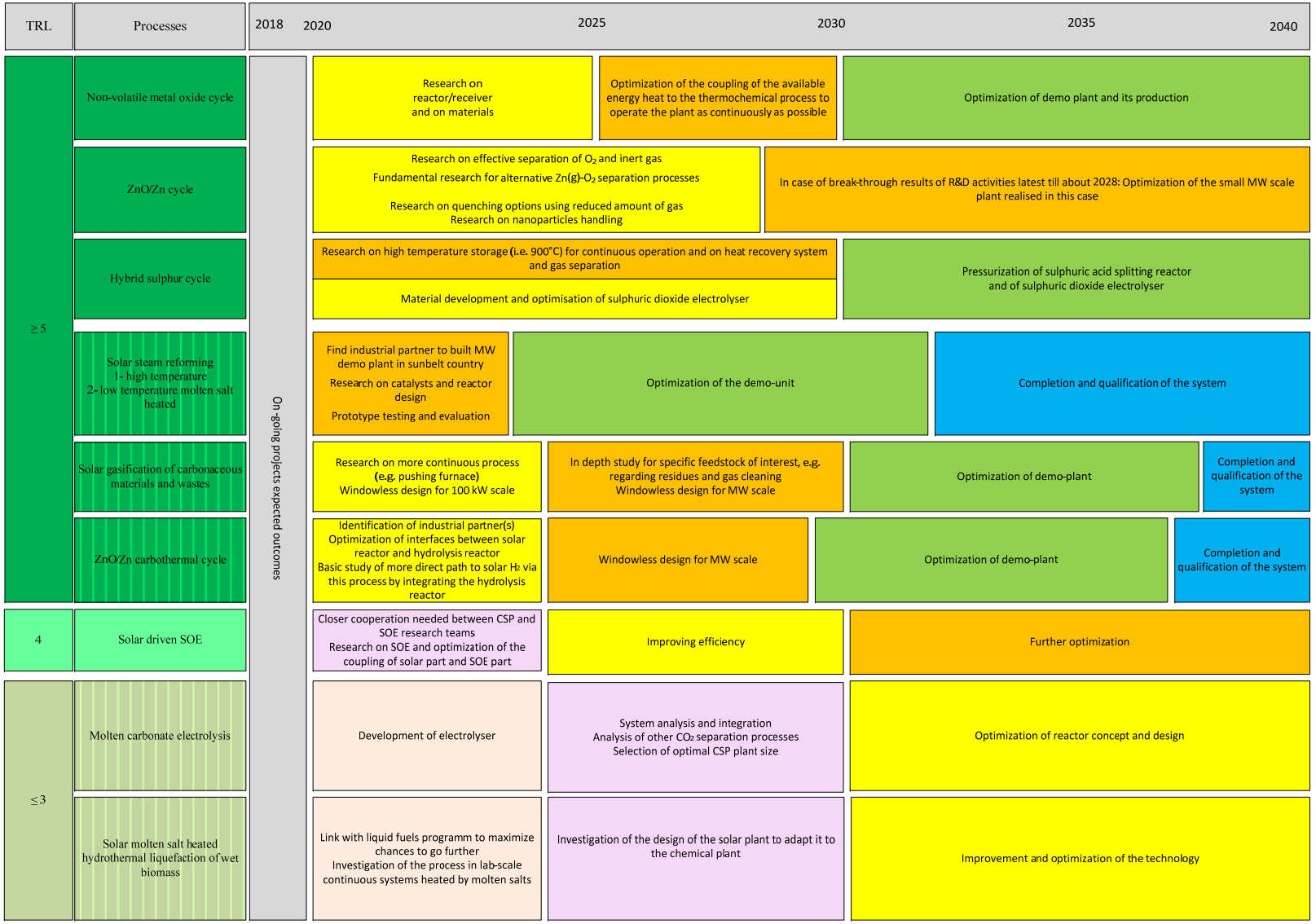

Figure 37. Summary of the R&D Strategy Roadmap.

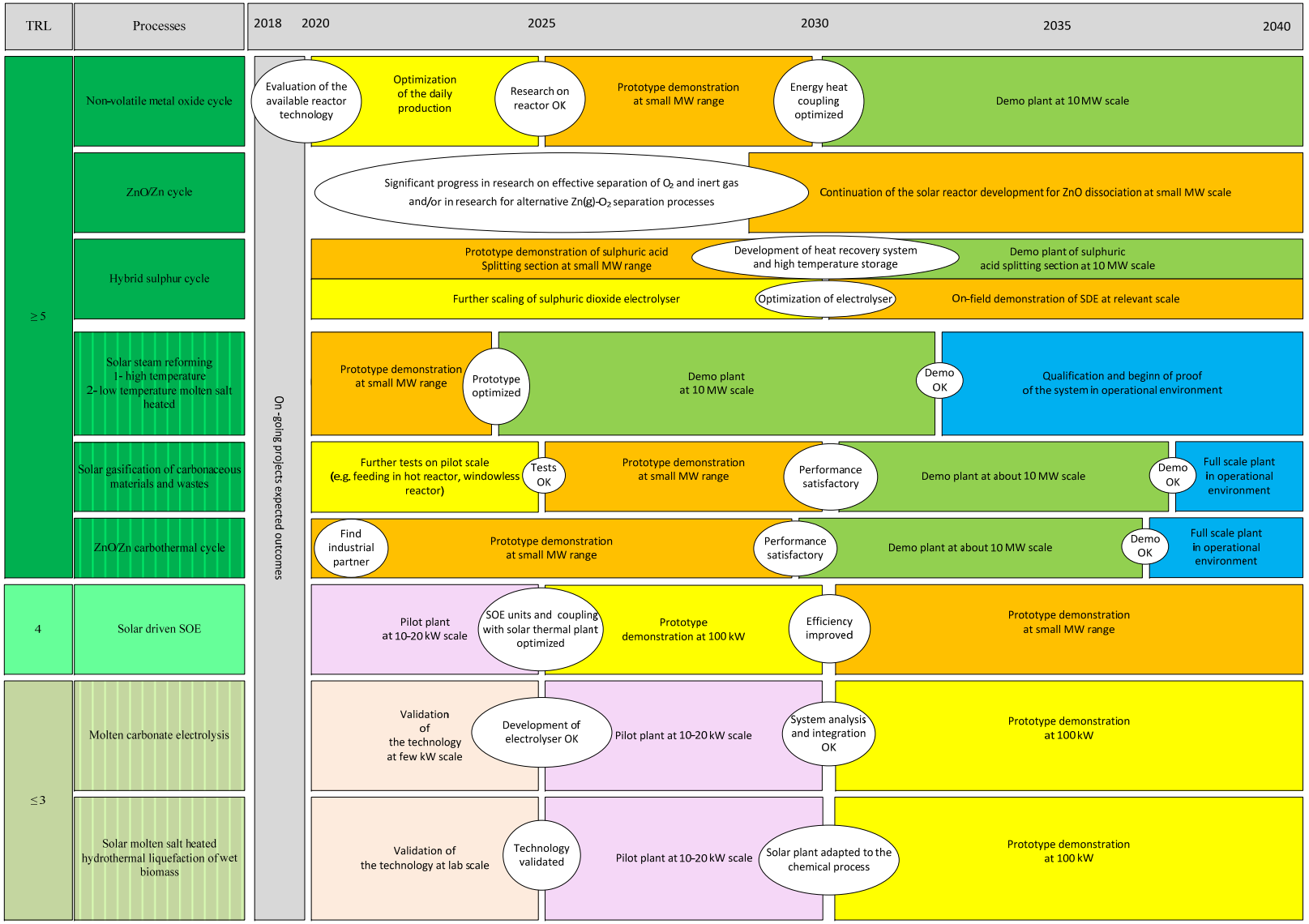

Figure 38. Summary of the Scale-up Strategy Roadmap.

5.3 References for Chapter 5

1. M. Romero, A. Steinfeld: Concentrating solar thermal power and thermochemical fuels, Energy & Environmental Science **5**(11), 9234, 2012.
2. A. Steinfeld: Solar hydrogen production via a two-step water-splitting thermochemical cycle based on Zn/ZnO redox reactions, International Journal of Hydrogen Energy **27**(6), 611-619, 2002.
3. R. Felder, A. Meier: Well-to-wheel analysis of solar hydrogen production and utilization for passenger car transportation, J. Solar Energy Engineering 130, 011017-1 – 011017-10, 2008.
4. A. Meier: Life cycle analysis and economic assessment of solar hydrogen, in Handbook of Hydrogen Energy, D.Y.G. S.A. Sherif, E.K. Stefanakos, A. Steinfeld, CRC Press Editor 2014, Chapter 14, 537-563. ISBN: 978-1-4200-5447-7
5. P. Charvin et al.: Analysis of solar chemical processes for hydrogen production from water splitting thermochemical cycles, Energy Conversion Management **49**, 1547–1556, 2008.
6. M. Kromer et al., Support for cost analyses on solar-driven high temperature thermochemical water-splitting cycles, in DE-DT0000951, Final Report to Department of Enerrgy, by TIAX, *LLC*2011: Lexington, MA, U.S.A.
7. J. Martinek et al.: Considerations for the design of solar-thermal chemical processes, Journal of Solar Energy Engineering **132**, 031013-1 - 031013-6, 2010.
8. J. Haltiwanger, J. Davidson, E. Winston: Renewable hydrogen from the Zn/ZnO solar thermochemical cycle: a cost and policy analysis, J. Solar Energy Eng. **132**, 041011-1 - 041011-8, 2010.
9. R. Jakober, E. Koepf et al.: Technoeconomic Analysis of industrial plant for H2 production via the ZnO/Zn solar thermochmical cycle, under preparation 2018.
10. R. Felder: Well-to-wheel analysis of renewable transport fuels: synthetic natural gas from wood gasification and hydrogen from concentrated solar energy, ETH Zürich, Doctoral Thesis No. 17437, 2007.
11. S. Kräupl, C. Wieckert: Economic evaluation of the solar carbothermic reduction of ZnO by using a single sensitivity analysis and a Monte-Carlo risk analysis, Energy **32**(7), 1134-1147, 2007.
12. E. Koepf et al.: A review of high temperature solar driven reactor technology: 25 years of experience in research and development at the Paul Scherrer Institute, Applied Energy **188**, 620-651, 2017.
13. A. G. Niehoff et al.: Process modelling and heat management of the solar hybrid sulfur cycle, Int. J. of Hydrogen Energy **40(**13), 4461-4473, 2015.
14. R. Liberatore et al.: Integration of photovoltaic and concentrated solar thermal technologies for H_2 production by the hybrid sulfur cycle. AIP Conference Proceedings **1850**, 1000132, 2017.

15. S. Möller et al.: Solar production of syngas for electricity generation: SOLASYS project test-phase, in Proceedings 11th SolarPACES Int. Symposium on Concentrated Solar Power and Chemical Energy Technologies, Zürich, Nov. 4-6, 2002.

16. S. Möller, D. Kaucic, C. Sattler: Hydrogen production by solar reforming of natural gas: A comparison study of two possible process configurations, J. Solar Energy Engineering **128**, 16-23, 2006.

17. European project MATS - Multipurpose Applications by Thermodynamic Solar, Contract n° 268219.

18. *http://cordis.europa.eu/result/rcn/192700_en.html*.

19. N. Monnerie et al.: Hydrogen production by coupling pressurized high temperature electrolyser with solar tower technology. Int. J. of Hydrogen Energy **42**, 13498-13509, 2017.

20. R. Zaetta, X. B. Madden: Hydrogen fuel cell bus technology state of the art review, 2011.

21. N. Piatkowski et al.: Solar-driven gasification of carbonaceous feedstock - a review. Energy & Environmental Science **4**(1), 73–82, 2011.

22. C. Jazrawi et al.: Pilot plant testing of continuous hydrothermal liquefaction of microalgae, Algal Research **2**, 268–277, 2013.

23. B. Patel, K. Hellgardt: Hydrothermal upgrading of algae paste in a continuous flow reactor, Bioresource Technology **191,** 460–468, 2015.

24. A.R. Suesse, G.A. Norton, J.v. Leeuwen: Pilot-scale continuous-flow hydrothermal liquefaction of filamentous fungi, Energy Fuels **30**, 7379−7386, 2016.

25. J. Reimer et al.: A novel salt separator for the supercritical water gasification of biomass, J. of Supercritical Fluids **117**, 113-121, 2016.

26. C. Wieckert, N. Tzouganatos, A.Steinfeld: Demonstration of a 5kW$_{th}$ windowless packed-bed reactor for high temperture solar thermochemical processing, in SolarPaces Conference 2017, Santiago de Chile, (anticipated) publication in AIP conference series, 2018.

6. Concluding remarks and outlook

A large number of research activities have been performed in WP9 of STAGE-STE with the goal to advance the knowledge for promising new technologies and to prepare for them further development steps towards higher TRL-levels.

A major achievement is the formulation of a technology roadmap which has been formulated in the Deliverable report D9.4 (see Figures 37 and 38). It is based on many findings generated mostly within STAGE-STE.

These activities and achievements became possible through an increased cooperation between the partners. This cooperation will surely be continued in the framework of the EERA JP CSP with its Subprogramme on “Solar driven thermochemical processes” and provides a sound basis for further fruitful cooperation in other projects.